Leukemia (2019) 33:249–278
https://doi.org/10.1038/s41375-018-0192-z

BRIEF COMMUNICATION

Chronic myelogenous leukemia

Dnmt1 links *BCR-ABLp210* to epigenetic tumor stem cell priming in myeloid leukemia

Carolina Vicente-Dueñas[1] · Inés González-Herrero[1,2] · Lalit Sehgal[3] · Idoia García-Ramírez[1,2] · Guillermo Rodríguez-Hernández[1,2] · Belén Pintado[4] · Oscar Blanco[1,5] · Francisco Javier García Criado[1,6] · María Begoña García Cenador[1,6] · Michael R. Green[3,7,8] · Isidro Sánchez-García[1,2]

Received: 17 April 2018 / Revised: 20 May 2018 / Accepted: 30 May 2018 / Published online: 28 June 2018

The clonal nature of cancer evolution dictates that all tumor cells carry the same cancer-initiating genetic lesions. However, the latest findings have shown that the mode of action of oncogenes is not homogeneous throughout the developmental history of the tumor. Studies on different types of hematopoietic and solid tumors have shown that the contribution of some oncogenes to cancer development is mediated through the epigenetic reprogramming of the cancer-initiating target cell [1–4]. Epigenetic reprogramming is therefore a new type of interaction between oncogenes and tumor cells, in which the oncogene primes for cancer development by establishing a new pathological tumor cell identity. The current challenge is to test whether epigenetic remodeling in the absence of the driver oncogene is sufficient for tumorigenesis.

Chronic myeloid leukemia (CML) is a malignancy of hematopoietic stem cells (HSCs) that harbor the Philadelphia (Ph) chromosome [5] and leads to increased abundance of myeloid cells and other non-lymphoid lineages in the blood and bone marrow. The Ph translocation creates the BCR-ABL fusion protein, with nearly all CML patients harboring a breakpoint that results in a 210-kD protein (*BCR-ABLp210*). This oncogene alone is capable of transforming hematopoietic progenitors and inducing CML [5]. The BCR-ABL protein is a constitutively active kinase that can be directly targeted with ABL-specific kinase inhibitors, such as Imatinib. The introduction of these agents that specifically target the cancer-initiating oncogene was a breakthrough in the clinical management of CML. However, treatment with Imatinib or other second-generation ABL kinase inhibitors is not curative and the disease returns upon cessation of the drug or the development of resistance. This is because CML stem cells are not dependent on BCR-ABL activity [6], suggesting that there may be an oncogenic function of *BCR-ABLp210* that can persist following inhibition of ABL kinase activity. In support of this notion, we have previously shown that the transient expression of *BCR-ABLp210* restricted to the hematopoietic stem/progenitor cell (HSPC) compartment of mice is capable of inducing mature myeloid leukemia [7]. In addition, we have also demonstrated that the expression of other oncogenes, such as *Bcl6*, within the HSPC compartment can reprogram HSPCs toward malignancy by fueling epigenetic changes that can be traced from the HSPCs to the malignant cells

These authors contributed equally: Carolina Vicente-Dueñas, Inés González-Herrero.

These authors jointly supervised this work: Michael R. Green, Isidro Sánchez-García.

Electronic supplementary material The online version of this article (https://doi.org/10.1038/s41375-018-0192-z) contains supplementary material, which is available to authorized users.

✉ Michael R. Green
MGreen5@mdanderson.org

✉ Isidro Sánchez-García
isg@usal.es

1 Institute of Biomedical Research of Salamanca (IBSAL), Salamanca, Spain

2 Experimental Therapeutics and Translational Oncology Program, Instituto de Biología Molecular y Celular del Cáncer, CSIC-USAL, Campus M. de Unamuno s/n, Salamanca, Spain

3 Department of Lymphoma/Myeloma, University of Texas MD Anderson Cancer Center, Houston, TX, USA

4 Transgenesis Facility CNB-CBMSO, CSIC-UAM, Madrid, Spain

5 Departamento de Anatomía Patológica, Universidad de Salamanca, Salamanca, Spain

6 Departamento de Cirugía, Universidad de Salamanca, Salamanca, Spain

7 Department of Genomic Medicine, University of Texas MD Anderson Cancer Center, Houston, TX, USA

8 Center for Cancer Epigenetics, University of Texas MD Anderson Cancer Center, Houston, TX, USA

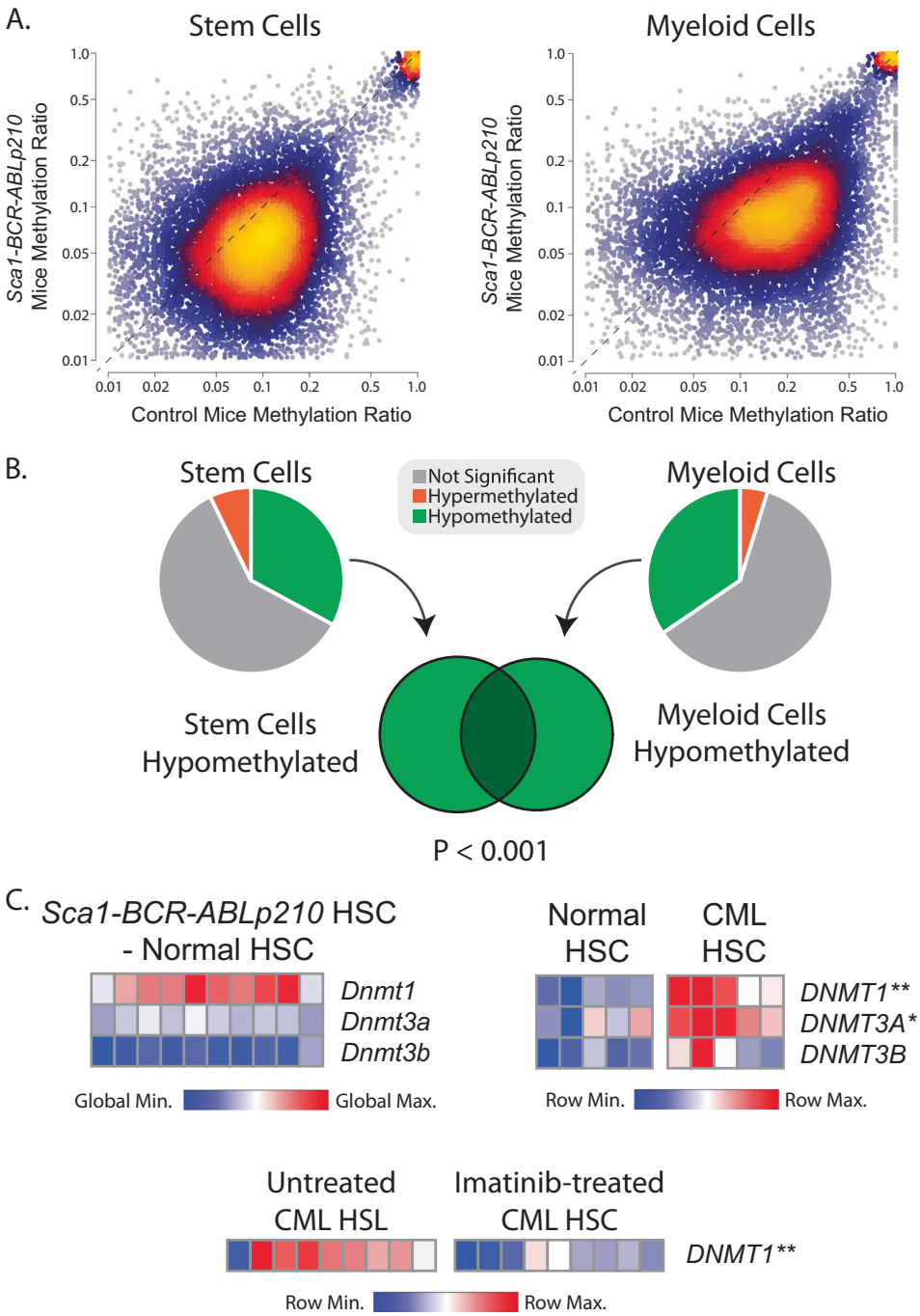

Fig. 1 Global hypomethylation and *DNMT1* overexpression associated with BCR-ABL oncogene expression in hematopoietic stem cells (HSCs). **a** Heat scatter plots show RRBS methylation profiling data from the HSPCs (Sca1+Lin−) of wild-type mice compared to those from *Sca1-BCR-ABLp210* transgenic mice (left) and from mature myeloid cells of wild type compared to *Sca1-BCR-ABLp210* mice (right). A significant and global loss of DNA methylation can be observed in the HSPCs and myeloid cells from *Sca1-BCR-ABLp210* mice. **b** Pie graphs and a Venn diagram illustrate that the majority of the changes in DNA methylation in each cellular compartment were hypomethylation, and the regions of hypomethylation significantly overlapped in HSPCs and mature myeloid cells. **c** Heat maps show the expression of DNA methyltransferases in murine and human HSCs. The relative expression of *Dnmt1*, but not other DNA methyltransferases, is higher in HSC from *Sca1-BCR-ABLp210* transgenic mice compared to wild-type mice (top left) and in HSC from CML patients compared to those from healthy donors (top right). The expression of *DNMT1* in HSC from CML patients is significantly reduced by BCR-ABL inhibition (bottom). $*P < 0.05$, $**P < 0.01$

[1]. These observations led us to hypothesize that *BCR-ABLp210* may function, in part, via epigenetic mechanisms that prime the tumor stem cell for malignant myeloid differentiation.

In order to investigate epigenetic reprogramming by the *BCR-ABLp210* oncogene, we performed reduced-representation bisulfite sequencing to interrogate the DNA methylation landscape in HSPCs (Sca1+Lin−) from wild-type and *Sca1-BCR-ABLp210* transgenic mice. The methods for all experiments are described in detail in supplementary information. This revealed a broad and significant loss of methylation at CpG islands that have a low-to-moderate level of methylation in wild-type HSPCs (Fig. 1a, Table S1). Importantly, this hypomethylation phenotype was conserved in mature myeloid cells from *Sca1-BCR-ABLp210* mice, despite the absence of the *BCR-ABLp210* oncogene in these cells (Fig. 1a, b, Table S2). This shows that transient HSPC-restricted expression of the *BCR-ABLp210* oncogene is capable of inducing significant

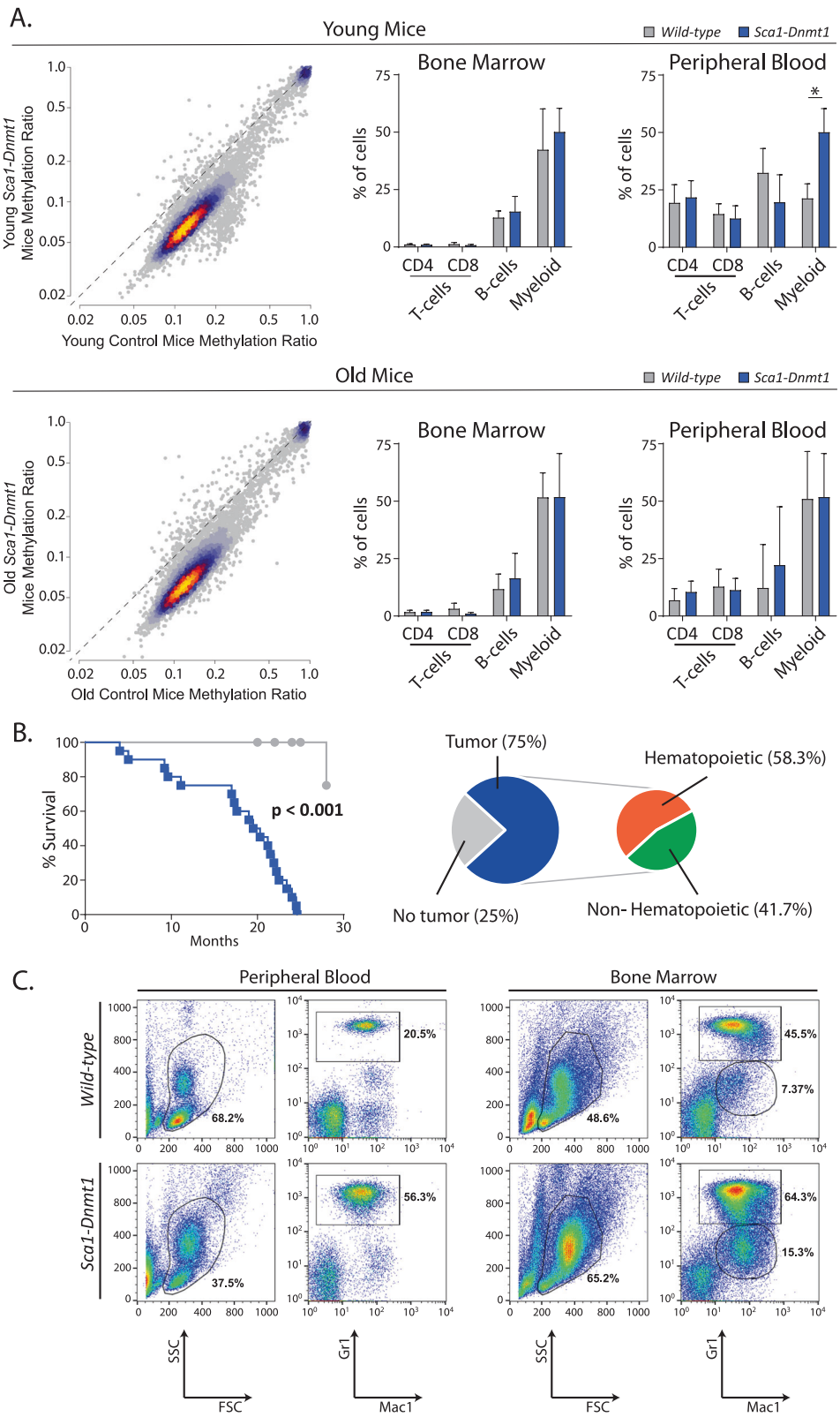

Fig. 2 Global hypomethylation and myeloid malignancies induced by *Dnmt1* expression in hematopoietic stem cells. **a** Heat scatter plots show the methylation ratio of CpG islands in the HSPCs from young (top) or old (bottom) wild-type control mice compared to those from young *Sca1-Dnmt1* mice. A clear loss of methylation can be observed in regions with a normally low-to-moderate level of methylation (0.1–0.2) in control mice. Bar graphs summarize the percentage of major hematological populations, interrogated by flow cytometry of bone marrow and peripheral blood of young (top) and old (bottom) wild-type and *Sca1-Dnmt1* mice. No significant differences were observed in the bone marrow at either time point. A significantly increase in the percentage of myeloid cells was observed in the peripheral blood of young disease-free *Sca1-Dnmt1* mice compared to their wild-type counterparts (*T* test *P* value < 0.001), but this was not observed in older mice. **b** Kaplan–Meier plot shows a significant reduction in survival of *Sca1-Dnmt1* mice (blue) compared to their wild-type counterparts (gray). Pie graphs summarize the necropsy results from *Sca1-Dnmt1* mice, with 75% of animals bearing tumors that were primarily of hematopoietic origin. **c** An illustrative example of flow cytometry of diseased *Sca1-Dnmt1* mice compared to age-matched controls shows the expansion of $Gr1^{+}Mac1^{+}$ myeloid cells in the blood and bone marrow, as well as the appearance of an abnormal $Gr1^{low}Mac1^{+}$ population in the bone marrow

and lasting changes in DNA methylation that may underlie stem cell reprogramming.

Prior studies have shown that DNA methyltransferase (DNMT) genes, including *DNMT1*, are aberrantly over-expressed in myeloid leukemias [8]. In line with this, gene

expression profiling (GEP) data from HSPCs of *Sca1-BCR-ABLp210* mice compared to those from wild-type mice [7] showed upregulation of *Dntm1* and downregulation of *Dnmt3b* expression, with no change in *Dnmt3a* expression (Fig. 1c). Higher expression of *DNMT1* was also observed in GEP data from human CML stem cells compared to normal HSCs [9] (*T* test *P* value = 0.003; Fig. 1c). The expression of *DNMT3A* was also significantly higher (*T* test *P* value = 0.012). Furthermore, GEP data from untreated and Imatinib-treated bone marrow cells of CML patients [10] showed that inhibition of BCR-ABL significantly reduces *DNMT1* expression (*T* test *P* value = 0.0004; Fig. 1c). Together these data show that *BCR-ABLp210* expression is associated with overexpression of *DNMT1* in both murine and human HSCs and that its expression may be linked to the activity of this oncogene.

The deregulation of DNA methylation by somatic mutations is one of the hallmarks of acute myeloid leukemia. Mutations of *IDH1*, *IDH2*, or *TET2*, function in the same pathway and inhibit the active and passive recycling of 5-methylcytosine to cytosine thereby inducing global hypermethylation. In contrast, mutations of the de novo methyltransferase, *DNMT3A*, function as dominant negative to inhibit the formation of DNMT3A homotetramers that efficiently methylate cytosine and leads to global hypomethylation. The DNMT3A protein performs its role as a de novo methyltransferase following its recruitment by other transcriptionally repressive complexes such as the polycomb repressor 2 (PRC2) complex [11]. DNMT1, DNMT3A, and DNTM3B have each been shown to interact with a similar region of the catalytic subunit of PRC2, EZH2 [11]. It is therefore plausible that overexpression of DNMT1 may sterically hinder the association between EZH2 and DNMT3A. The loss of only a single allele of *Dnmt3a* is sufficient to promote myeloid leukemia in mice, despite causing only modest changes in DNA methylation [12], demonstrating that slight perturbations in Dnmt function are sufficient for leukemogenesis. Human CML also shows disordered DNA methylation [13], but the mechanism for this has not been defined. Deregulation of this axis is therefore clearly important for myeloid malignancies. But there is still not a clear understanding of specific genes or pathways that contribute to myeloid transformation as a result of perturbations in DNA methylation. Our observations therefore led us to investigate whether *Dnmt1* overexpression was mechanistically linked with perturbed DNA methylation and myeloid leukemogenesis.

Transient expression of *BCR-ABLp210* in HSPCs was sufficient to promote myeloid leukemia, and Imatinib treatment leads to downregulation of *Dnmt1* but does not eradicate the disease. We therefore hypothesized that transient expression of *Dnmt1* would also be sufficient for stem cell reprogramming, and we modeled this by expressing *Dnmt1* under control of the endogenous *Sca1* promoter for HSPC-restricted expression (Figs. S1–2). Notably, the expression of *Dnmt1* resulted in DNA hypomethylation in HSPCs similar to that observed in *Sca1-BCR-ABLp210* mice, with the most notable changes at loci with normally low/moderate levels of methylation (Fig. 2a, Table S3). No significant alterations were observed in the frequencies of major hematologic subsets in the bone marrow of young *Sca1-Dnmt1* mice (3–7 months), but there was a significant expansion of myeloid cells in the peripheral blood compared to wild-type mice (Fig. 2a). Although the DNA hypomethylation phenotype persisted in the HSPCs of older mice (16–24 months, Fig. 2a, Table S4), there was no significant difference in myeloid cells in either the bone marrow or the peripheral blood at this stage. The HSPC-restricted expression of *Dnmt1* is therefore capable of phenocopying the pattern of lasting DNA hypomethylation that was observed in *BCR-ABLp210* mice.

Aging *Sca1-Dnmt1* mice had a shorter lifespan than wild-type mice due to the development of cancer, the majority of which were myeloid malignancies (Fig. 2b). The *Sca1-Dnmt1* mice that developed myeloid malignancies showed marked expansion of $Mac1^{+}Gr1^{+}$ granulocytes in the blood and bone marrow (Fig. 2c and S3), as well as the presence of an abnormal myeloid population ($Mac1^{+}Gr1^{low}$) in the bone marrow (Fig. 2c). This was also associated with a loss of normal architecture in the spleen (Fig. S4), with tumor-bearing *Sca1-Dnmt1* mice showing atrophic white pulp and hyperplasic red pulp infiltrated by myeloid cells. In the liver, tumor infiltration was accompanied by deposition of an eosinophilic hyaline substance (Fig. S4). A prior study showed that the expression of a hypomorphic *Dnmt1* allele induced global DNA hypomethylation and led to tumors in mice [14], potentially via the promotion of chromosomal instability resulting from the reactivation of endogenous retroviral elements [15]. We did not observe the expression of the *Cdkn2a* ($p19^{Arf}$) gene in bone marrow cells from *Sca1-Dnmt1* mice, indicating the absence of oncogenic stress resulting from chromosome instability (data not shown). Together, these data show that HSPC-restricted expression of *Dnmt1* is sufficient to phenocopy the DNA hypomethylation phenotype induced by *BCR-ABLp210* expression in the same compartment and to promote the development of myeloid malignancies. The deregulation of DNA methylation alone is therefore sufficient to prime HSPCs for the development of myeloid leukemia.

In conclusion, here we have characterized epigenetic reprogramming linked to HSPC-restricted expression of *BCR-ABLp210*, which persists in myeloid cells despite the absence of the oncogene. We identified upregulation of *Dnmt1* as a consequence of *BCR-ABLp210*, and we show

that HSPC-restricted expression of *Dnmt1* in transgenic mice is sufficient to phenocopy the *BCR-ABLp210*-associated DNA methylation changes and induce myeloid malignancies. This provides, to our knowledge, the first experimental evidence that epigenetic tumor stem cell reprogramming by itself is sufficient to drive cancer development and establish the tumor cell identity. These observations provide important mechanistic insight into the epigenetic reprogramming of HSC by the *BCR-ABLp210* oncogene and the etiology of CML.

Acknowledgements We are indebted to all members of our groups for useful discussions and for their critical reading of the manuscript. Research in CVD group is partially supported by FEDER, "Miguel Servet" Grant (CP14/00082 - AES 2013-2016) from the Instituto de Salud Carlos III (Ministerio de Economía y Competitividad), "Fondo de Investigaciones Sanitarias/Instituto de Salud Carlos III" (PI17/00167), and by the Lady Tata International Award for Research in Leukaemia 2016–2017. Research in ISG group is partially supported by FEDER and by MINECO (SAF2012-32810, SAF2015-64420-R and Red de Excelencia Consolider OncoBIO SAF2014-57791-REDC), Instituto de Salud Carlos III (PIE14/00066), ISCIII- Plan de Ayudas IBSAL 2015 Proyectos Integrados (IBY15/00003), by Junta de Castilla y León (BIO/SA51/15, CSI001U14, UIC-017, and CSI001U16), and by the German Carreras Foundation (DJCLS R13/26). ISG lab is a member of the EuroSyStem and the DECIDE Network funded by the European Union under the FP7 program. IGR was supported by BES-Ministerio de Economía y Competitividad (BES-2013-063789). GRH was supported by FSE-Conserjería de Educación de la Junta de Castilla y León (CSI001-15).

Compliance with ethical standards

Conflict of interest The authors declare that they have no conflict of interest.

References

1. Green MR, Vicente-Duenas C, Romero-Camarero I, Long Liu C, Dai B, Gonzalez-Herrero I, et al. Transient expression of Bcl6 is sufficient for oncogenic function and induction of mature B-cell lymphoma. Nat Commun. 2014;5:3904.
2. Bartlett TE, Chindera K, McDermott J, Breeze CE, Cooke WR, Jones A, et al. Epigenetic reprogramming of fallopian tube fimbriae in BRCA mutation carriers defines early ovarian cancer evolution. Nat Commun. 2016;7:11620.
3. Fang D, Gan H, Lee JH, Han J, Wang Z, Riester SM, et al. The histone H3.3K36M mutation reprograms the epigenome of chondroblastomas. Science. 2016;352:1344–8.
4. Vicente-Duenas C, Romero-Camarero I, Gonzalez-Herrero I, Alonso-Escudero E, Abollo-Jimenez F, Jiang X, et al. A novel molecular mechanism involved in multiple myeloma development revealed by targeting MafB to haematopoietic progenitors. EMBO J. 2012;31:3704–17.
5. Sawyers CL. Chronic myeloid leukemia. N Engl J Med. 1999;340:1330–40.
6. Corbin AS, Agarwal A, Loriaux M, Cortes J, Deininger MW, Druker BJ. Human chronic myeloid leukemia stem cells are insensitive to imatinib despite inhibition of BCR-ABL activity. J Clin Invest. 2011;121:396–409.
7. Perez-Caro M, Cobaleda C, Gonzalez-Herrero I, Vicente-Duenas C, Bermejo-Rodriguez C, Sanchez-Beato M, et al. Cancer induction by restriction of oncogene expression to the stem cell compartment. EMBO J. 2009;28:8–20.
8. Mizuno S, Chijiwa T, Okamura T, Akashi K, Fukumaki Y, Niho Y, et al. Expression of DNA methyltransferases DNMT1, 3A, and 3B in normal hematopoiesis and in acute and chronic myelogenous leukemia. Blood. 2001;97:1172–9.
9. Gerber JM, Gucwa JL, Esopi D, Gurel M, Haffner MC, Vala M, et al. Genome-wide comparison of the transcriptomes of highly enriched normal and chronic myeloid leukemia stem and progenitor cell populations. Oncotarget. 2013;4:715–28.
10. Benito R, Lumbreras E, Abaigar M, Gutierrez NC, Delgado M, Robledo C, et al. Imatinib therapy of chronic myeloid leukemia restores the expression levels of key genes for DNA damage and cell-cycle progression. Pharmacogenet Genomics. 2012;22:381–8.
11. Vire E, Brenner C, Deplus R, Blanchon L, Fraga M, Didelot C, et al. The Polycomb group protein EZH2 directly controls DNA methylation. Nature. 2006;439:871–4.
12. Cole CB, Russler-Germain DA, Ketkar S, Verdoni AM, Smith AM, Bangert CV, et al. Haploinsufficiency for DNA methyltransferase 3A predisposes hematopoietic cells to myeloid malignancies. J Clin Invest. 2017;127:3657–74.
13. Heller G, Topakian T, Altenberger C, Cerny-Reiterer S, Herndlhofer S, Ziegler B, et al. Next-generation sequencing identifies major DNA methylation changes during progression of Ph+ chronic myeloid leukemia. Leukemia. 2016;30:1861–8.
14. Gaudet F, Hodgson JG, Eden A, Jackson-Grusby L, Dausman J, Gray JW, et al. Induction of tumors in mice by genomic hypomethylation. Science. 2003;300:489–92.
15. Howard G, Eiges R, Gaudet F, Jaenisch R, Eden A. Activation and transposition of endogenous retroviral elements in hypomethylation induced tumors in mice. Oncogene. 2008;27:404–8.

Leukemia (2019) 33:254–257
https://doi.org/10.1038/s41375-018-0194-x

Multiple myeloma gammopathies

Assay to rapidly screen for immunoglobulin light chain glycosylation: a potential path to earlier AL diagnosis for a subset of patients

Sanjay Kumar[1] · David Murray[2] · Surendra Dasari[3] · Paolo Milani[4] · David Barnidge[2] · Benjamin Madden[5] · Taxiarchis Kourelis[1] · Bonnie Arendt[2] · Giampaolo Merlini[4] · Marina Ramirez-Alvarado[6] · Angela Dispenzieri[1,2]

Received: 27 February 2018 / Revised: 1 May 2018 / Accepted: 21 May 2018 / Published online: 6 July 2018

Systemic light chain (LC) amyloidosis (AL) is a protein misfolding disease in which a monoclonal immunoglobulin LC self-aggregates to form insoluble amyloid fibrils, which deposit in different organs and impairs the physiology of organs [1]. Researchers postulated that glycosylation also has a pathogenic effect on LCs and glycosylated LCs could be more prone to be amyloidogenic [2]. Pathogenic glycosylation of proteins has been implicated in various hematological malignancies, often with prognostic implications [3]. However, in comparison with other diseases, glycosylation of LCs has been relatively underinvestigated in AL. This is largely due to the lack of a high-throughput procedure to facilitate rapid analysis of LC glycosylation.

Previous studies using immuno-enrichment-based matrix-assisted laser desorption ionization time-of-flight mass spectrometry (MALDI-TOF-MS), termed MASS-FIX, demonstrated that M-protein mass distributions from AL patients often had an additional "polytypic-like" pattern along with the diagnostic monoclonal LC [4]. Further studies using high-resolution liquid chromatography-based MS (LC-MS) suggested that posttranslational modifications such as glycosylation on LCs could produce this "polytypic-like" pattern in AL patients [5]. Using MS approaches, we provide the most comprehensive mapping of LC glycosylation in AL reported to date.

We obtained serum or plasma samples from total 311 patients and arranged them into two cohorts. The first cohort had 157 AL previously untreated patients who had their amyloid protein sequenced by LC-MS/MS [1]. The second cohort included 154 patients who had previously untreated AL ($n = 32$) or another diagnosis such as multiple myeloma ($n = 54$), Waldenstrom macroglobulinemia ($n = 8$), monoclonal gammopathy of undetermined significance ($n = 57$), and other plasma cell disorder (PCD) [4] (Table 1).

The immuno-enrichment was performed as previously described by adding 10 µL aliquot of serum to 20 µL agarose beads coupled with one of the single-domain antibodies specific for heavy chain (HC) of IgM, IgA, and IgG, and LC of κ or λ constant domains (Thermo Fischer Scientific), washed, reduced, spotted on MALDI target plate (Bruker), and analyzed separately on MALDI-TOF-MS (Microflex LT, Bruker) [4, 6]. The spectra from each five immuno-enrichment of each sample were overlaid and LC m/z distribution was visually inspected for the presence of peaks in $[M + 1\,H]^{1+}$ and $[M + 2\,H]^{2+}$ using Flex Analysis software (Bruker), and categorized patient's monoclonal LC as either "suspected-glycosylation or "no glycosylation" based on observed peak patterns.

Deglycosylation was executed to confirm suspected-glycosylation in monoclonal LC. Briefly, 10 µl of serum of suspected-glycosylation sample was mixed with 20 µl of either κ- or λ-specific beads, and incubated for 45 min at room temperature. After washing with phosphate-buffered

Electronic supplementary material The online version of this article (https://doi.org/10.1038/s41375-018-0194-x) contains supplementary material, which is available to authorized users.

✉ Angela Dispenzieri
Dispenzieri.Angela@mayo.edu

1 Division of Hematology, Mayo Clinic, Rochester, MN, USA

2 Department of Laboratory Medicine, Mayo Clinic, Rochester, MN, USA

3 Department of Health Science, Mayo Clinic, Rochester, MN, USA

4 Amyloidosis Research and Treatment Center, Fondazione IRCCS Policlinico San Matteo and Department of Molecular Medicine, University of Pavia, Pavia, Italy

5 Medical Genomics Facility, Proteomics Core, Mayo Clinic, Rochester, MN, USA

6 Departments of Biochemistry and Molecular Biology, Mayo Clinic, Rochester, MN, USA

Table 1 Distribution of MASS-FIX patterns for LCs in patients with AL vs. non-AL and serum-free LC measurements for glycosylated vs. non-glycosylated LC Shouldn't data in columns be cnetered like their headers are

	κ Clone	λ Clone	All patients
Sample type	**Suspected glycosylation by MASS-FIX**		
AL, *n*/*N* (%)	20/61 (32.8)	13/128 (10.2)	33/189 (17.5)
Non-AL, *n*/*N* (%)	3[a]/81 (3.7)	2[b]/41 (4.9)	5/122 (4.1)
P-value	< 0.001	NS	*P* < 0.001
Odds ratio	12.68	2.20	4.95
	Median FLC measurement, mg/dL (IQR)		
Glycosylated ($n = 36$)	34.4 (4.1–90.5)	50.8 (13.9–79)	–
Non-glycosylated ($n = 252$)	16.5 (3.1–90.5)	13.5 (3.8–45.1)	–
p-Value	NS	0.02	

[a]Diagnoses of these three patients included plasma cell leukemia ($n = 1$) and multiple myeloma ($n = 2$)

[b]Diagnoses of two patients were one each of MGUS and multiple myeloma.

AL, amyloidosis; IQR, interquartile range; FLC, free light chain; LC, light chain; MGUS, monoclonal gammopathy of undetermined significance; NS, not significant.

saline and water, the mixture were denatured and reduced with 100 µl of 2% SDS and 10 mM Tris (2-carboxyethyl) phosphine at 56 °C for 30 min with shaking. SDS was removed using DRS spin column (Thermo Fischer Scientific). The reduced LCs was treated with 1 µl of PNGase F (New England Biolab, Inc.) at 37 °C for 3 h with shaking. Reactions were stopped by adding 20 µl of 0.1% trifluoroacetic acid and analyzed on MALDI-TOF-MS.

The same suspected-glycosylation-LC samples were further analyzed on high-resolution LC-MS consisting of Orbitrap Elite (Thermo Fisher Scientific) coupled to an Ultimate 3000 HPLC system (Thermo Fisher Scientific) using ProSwift RP-4H capillary monolithic column (Thermo Fisher Scientific). The spectra were acquired in positive mode between 500 and 3000 m/z in Orbitrap, and analyzed using Xcalibur Qual Browser software (Thermo Fisher Scientific). The difference in mass of suspected-glycosylation-LC before and after PNGase F treatment was determined, and matched with mass of immunoglobulin *N*-glycans. All experiments were repeated in three replicates.

The differences between patient groups were calculated using Fisher's exact test (JMP 13 SAS, Carey, NC). The odds ratio for suspected-glycosylated-LC patient being AL was 12.68 for κ and 2.20 for λ (Table 1). This study was approved by the Mayo Clinic Institutional Review Board.

The mass spectra for all patients were classified into two mutually exclusive categories: suspected glycosylation ($n = 38$) and no glycosylation ($n = 273$) (Supplementary Figure 1). Suspected glycosylation LC presented as a broad peak in MS spectrum that was higher in mass than expected for LCs. Thirty-three percent of AL-κ patients had suspected-glycosylation pattern, compared with 10.2% of AL-λ patients. The rate of suspected-glycosylation LC among non-AL, κ, and λ patients was 3.7% and 4.9%, respectively (Table 1). Of the 38 patients with suspected-glycosylated LCs, 16 were LC-only patients and 22 patients had intact M-proteins along with their free LCs. Among the λ patients (Table 1), the λ free LC was higher in the suspected-glycosylated patients than the non-glycosylated patients, which could be a function of the assay's inability to detect glycosylation in a very small clone in a polyclonal background with the current immuno-enrichment methodology. Once LC beads become available as part of the pre-analytics and/or more urine samples are tested, there will likely be a greater ability to detect these patterns in smaller clones.

To confirm LC glycosylation, the subset of 21 κ (18 AL and 3 non-AL) and 9 λ (7 AL and 2 non-AL) suspected-glycosylation samples were analyzed using PNGase F on MALDI-TOF-MS. The LC spectra of all 30 samples shifted to a narrower and lower molecular mass after PNGase F as compared with native LC peak, in both $[M + 2\,H]^{2+}$ and $[M + 1\,H]^{1+}$ charged states, indicating *N*-glycosylation (Fig. 1a).

To further verify the MASS-FIX pattern represented *N*-glycosylation, 19 (13 κ and 6 λ) suspected-glycosylation-LC samples were studied by LC-MS using PNGase F; all samples demonstrated a shift toward lower molecular weight after PNGase F treatment, affirming that the broad peak patterns observed by MASS-FIX were a signature for glycosylated LCs. The difference in mass before and after PNGase F was matched with molecular weights of known *N*-glycans (Fig. 1b). Bi-antennary sialated *N*-glycan forms G2FNSA2 and G2FSA2 were observed in most cases, whereas others had fragments of these glycan groups (Supplementary Table 1).

As 158 patients had their LC gene sequence by tissue mass spectrometry [1], associations between immunoglobulin LC usage and the presence of glycosylation were sought. As shown in Fig. 1c, 41% of AL whose amyloid protein was of the KV1 gene family had glycosylated circulating LC. The κ-LCs derived from *KV1-33* and *KV1-39* were most represented (Fig. 1d). The λ gene family most represented was LV3, with *LV3-21* having the highest likelihood of being glycosylated.

Until now, a limited number of patients had been studied to investigate *N*-glycosylation of LCs in AL [7, 8]. In 2000, Stevens [9] summarized the glycosylation literature. Only 9 of 22 λ-LC proteins exhibiting potential glycosylation sites

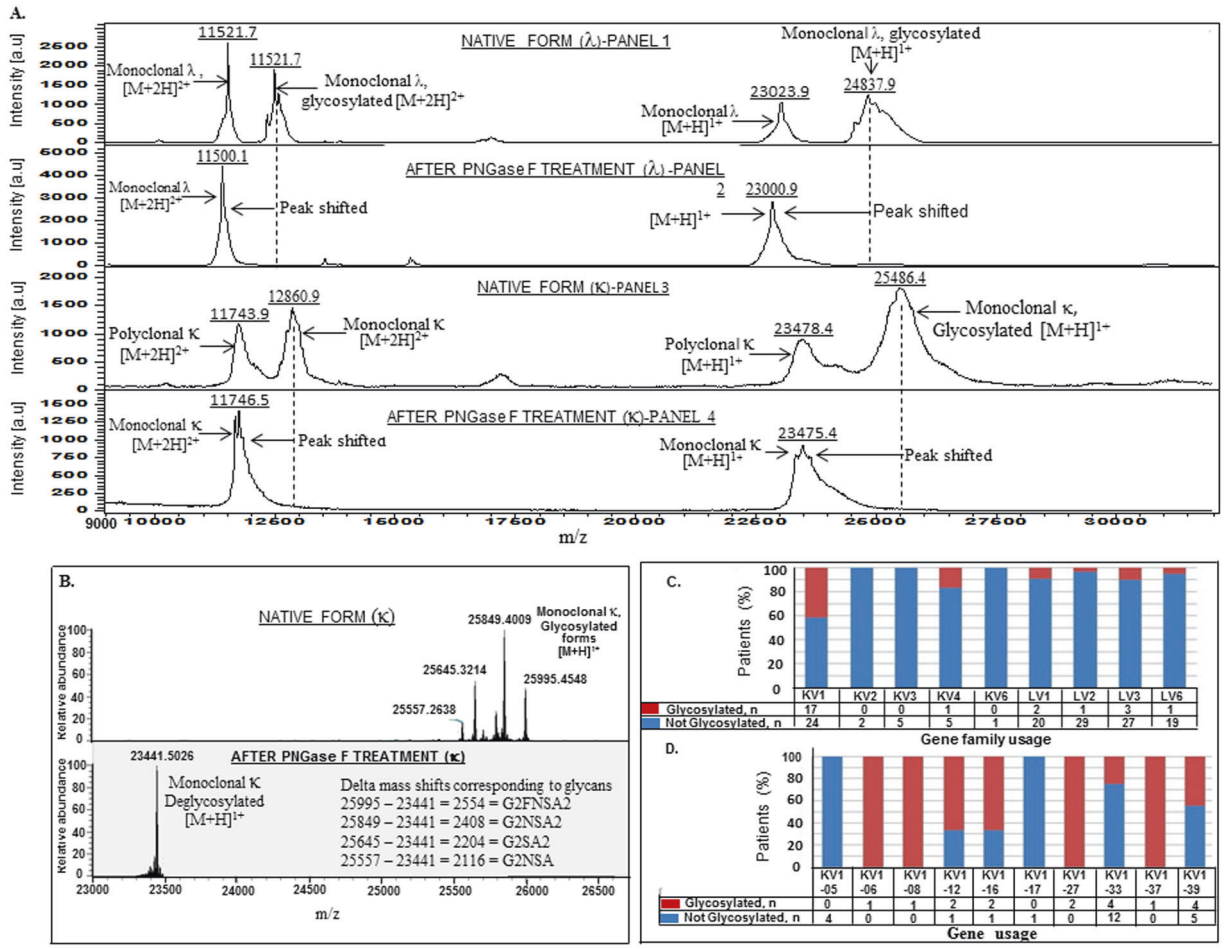

Fig. 1 **a** Deglycosylation of monoclonal light chain with PNGase F. Glycosylated monoclonal λ and κ, LC in native form (panel 1 and 3), and PNGase F treatment showing shift with reduced molecular weight toward unglycosylated form (panel 2 and 4). **b** Monoclonal κ, light chain glycosylation analysis by high-resolution LC-MS. There were at least four peaks representing different glycoforms of monoclonal κ light chain (upper panel). After PNGase F treatment, monoclonal κ light chain is resolved to a single peak of 23,441 Da (lower panel). The difference in molecular weight of peak before and after PNGase F was matched with molecular weight of different glycans as G2FNSA2, G2NSA2, G2SA2, and G2NSA mentioned in Supplementary Table 1. **c** Immunoglobulin LC gene usage based on the presence or absence of LC glycosylation. Gene family and gene usage was determined by bottom-up sequencing of amyloid from tissue biopsy [11]. By gene family: KV1 and KV4 gene families had highest rates of glycosylation. **d** A closer look at the KV1 gene family: 25% of *KV1-33* and 41% of *KV1-39* patients' monoclonal serum immunoglobulin light chains were glycosylated

were from AL patients. In contrast, 18 of 22 potentially glycosylated KV1, LCs were from AL patients despite the fact that germline KV1 genes do not encode for N-linked glycosylation motif (N-*x*-S/T) [9]. It is noteworthy that we have observed that 8.5% (81/948) of KV1 mRNA sequences of various PCDs including AL derived from a LC sequence database had an *N*-glycosylation motif [10]. These results suggest somatic hypermutation affinity maturation of κ-LCs generates *N*-glycosylation sites (N-*x*-S/T). *N*-glycosylation has been reported in κ-LCs from urine in two AL patients, who had consensus glycosylation sequence (N-*x*-S/T) in germline using chromatography and MALDI-TOF-MS [11], but chromatography is analytically complex, cumbersome, and time consuming, making it unsuitable for routine clinical use. In contrast, our novel MASS-FIX method easily and rapidly characterizes LC glycosylation.

Several studies have described carbohydrate moieties in their LC of patients with PCDs; [12] it was recognized that 4% (3/71) of Bence Jones proteins from myeloma patients' urine and 11% (2/18) of LCs from multiple myeloma serum had carbohydrate moieties attached [13]. Prior studies identified sialic acid, *N*-acetyl-glucsosamine, *N*-acetyl-galactosamine, and other "neutral sugars" attached to LCs [13]. Approximately 15% of immunoglobulin LCs in circulation have been shown to have oligosaccharides [13]. In the present study, the most common *N*-glycans were found to be G2FNSA2 and G2FSA2 as bi-antennary and sialated, which supports the previous study that LCs are highly sialylated [14, 15]. Despite the disparity of frequency of *N*-glycosylation for κ and λ-LCs, the composition of *N*-glycans did not appear to be different.

In summary, we identified *N*-glycosylation in the serum LCs of one-third of κ-AL and 10% of λ-AL patients. The novelty of our work is the application of a quick, inexpensive, high-throughput method to identify LC *N*-glycosylation, i.e., MASS-FIX. Although this finding will apply to only 11% of AL cases (one-third of AL cases are κ and one-third of κ-AL are glycosylated), we anticipate that over the next decade, MASS-FIX will replace immunofixation as a screen for monoclonal proteins, providing both information on isotype for all patients and AL risk in a subset. Moreover, with better immune-enrichment, the twofold higher rate of glycosylation observed in λ-AL cases over other PCDs may become significant, further increasing the value of this method to prompt clinicians to have a higher suspicion for AL in an even higher proportion of patients.

Acknowledgements We thank MeLea Hetrick and Mindy Kohlhagen for their help during experiments. This research was supported by Mayo Clinic, Rochester, MN, USA. This work was in part supported by the Predolin Foundation, the JABBS Foundation, a generous donation in the memory of Joey Bartzis, and by NIH grant CA125614.

Author contributions: SK performed the experiments and drafted the manuscript. SK, AD, DLM, and SD designed, analyzed, interpreted the data, and edited the manuscript. BM performed the LC-MS experiments. PM had performed the experiments on the 154 patients from a prior report. TK and SD had performed the analyses of tissue amyloid as per a prior publication. Other authors contributed intellectual content and review of this manuscript.

Compliance with ethical standards

Conflict of interest DLM and SD have financial interest in the MASS-FIX technology used in this study. All other authors declare that they have no conflict of interest.

References

1. Kourelis TV, Dasari S, Theis JD, Ramirez-Alvarado M, Kurtin PJ, Gertz MA, et al. Clarifying immunoglobulin gene usage in systemic and localized immunoglobulin light-chain amyloidosis by mass spectrometry. Blood. 2017;129:299–306.
2. Bellotti V, Mangione P, Merlini G. Review: immunoglobulin light chain amyloidosis--the archetype of structural and pathogenic variability. J Struct Biol. 2000;130:280–9.
3. Pinho SS, Reis CA. Glycosylation in cancer: mechanisms and clinical implications. Nat Rev Cancer. 2015;15:540–55.
4. Milani P, Murray DL, Barnidge DR, Kohlhagen MC, Mills JR, Merlini G, et al. The utility of MASS-FIX to detect and monitor monoclonal proteins in the clinic. Am J Hematol. 2017;92:772–9.
5. Barnidge DR, Dispenzieri A, Merlini G, Katzmann JA, Murray DL. Monitoring free light chains in serum using mass spectrometry. Clin Chem Lab Med. 2016;54:1073–83.
6. Kohlhagen MC, Barnidge DR, Mills JR, Stoner J, Gurtner KM, Liptac AM, et al. Screening method for M-proteins in serum using nanobody enrichment coupled to MALDI-TOF mass spectrometry. Clin Chem. 2016;62:1345–52.
7. Dwulet FE, O'Connor TP, Benson MD. Polymorphism in a kappa I primary (AL) amyloid protein (BAN). Mol Immunol. 1986;23:73–8.
8. Toft KG, Sletten K, Husby G. The amino-acid sequence of the variable region of a carbohydrate-containing amyloid fibril protein EPS (immunoglobulin light chain, type lambda). Biol Chem Hoppe Seyler. 1985;366:617–25.
9. Stevens FJ. Four structural risk factors identify most fibril-forming kappa light chains. Amyloid. 2000;7:200–11.
10. Dasari S, Theis JD, Vrana JA, Meureta OM, Quint PS, Muppa P, et al. Proteomic detection of immunoglobulin light chain variable region peptides from amyloidosis patient biopsies. J Proteome Res. 2015;14:1957–67.
11. Connors LH, Jiang Y, Budnik M, Theberge R, Prokaeva T, Bodi KL, et al. Heterogeneity in primary structure, post-translational modifications, and germline gene usage of nine full-length amyloidogenic kappa1 immunoglobulin light chains. Biochemistry. 2007;46:14259–71.
12. Sletten KWP, Husby G. Structural studies of the variable region of immunoglobulin light chain type amyloid fibril proteins. In: Glenner GGOE, Bendit EP, Calkins E, Cohen AS, Zucker-Franklin D, (ed). Amyloidosis. New York: Plennum Press; 1986. p. 463–75.
13. Sox HC Jr., Hood L. Attachment of carbohydrate to the variable region of myeloma immunoglobulin light chains. Proc Natl Acad Sci USA. 1970;66:975–82.
14. Ohkura T, Isobe T, Yamashita K, Kobata A. Structures of the carbohydrate moieties of two monoclonal human lambda-type immunoglobulin light chains. Biochemistry. 1985;24:503–8.
15. Youings A, Chang SC, Dwek RA, Scragg IG. Site-specific glycosylation of human immunoglobulin G is altered in four rheumatoid arthritis patients. Biochem J. 1996;314(Pt 2):621–30.

Leukemia (2019) 33:258–261
https://doi.org/10.1038/s41375-018-0195-9

Multiple myeloma gammopathies

Bortezomib-based induction therapy with high or low-dose dexamethasone in newly diagnosed, transplant-eligible multiple myeloma

Elias K. Mai[1] · Thomas Hielscher[2] · Uta Bertsch[1] · Jana Schlenzka[1] · Hans J. Salwender[3] · Markus Munder[4] · Christian Gerecke[5] · Ulrich Dührsen[6] · Peter Brossart[7] · Kai Neben[8] · Jens Hillengass[1] · Marc S. Raab[1] · Maximilian Merz[1] · Marc-Andrea Baertsch[1] · Anna Jauch[9] · Dirk Hose[1] · Hans Martin[10] · Hans-Walter Lindemann[11] · Igor W. Blau[12] · Christof Scheid[13] · Katja C. Weisel[14] · Hartmut Goldschmidt[1,15] · for the German-speaking Myeloma Multicenter Group (GMMG)

Received: 5 April 2018 / Revised: 8 May 2018 / Accepted: 15 May 2018 / Published online: 29 June 2018

The advent of novel agents in the treatment of multiple myeloma (MM) improved disease control, survival and reduced toxicities. However, as demonstrated by the study from Rajkumar et al. [1], accompanying steroid therapy is also of critical importance in newly diagnosed MM (NDMM). In their phase III trial, Rajkumar et al. Compared lenalidomide (LEN) with either high (40 mg on days 1–4, 9–12, 17–20; 480 mg per cycle) or low (40 mg on days 1, 8, 15, 22; 160 mg per cycle) dose dexamethasone (DEX) in both transplant-eligible and -ineligible NDMM. The trial was stopped prematurely after one year due to a significant difference in overall survival (OS), favoring the low-dose DEX arm (96 vs. 87%, $p < 0.001$). This difference was caused by an increased rate in early mortality and toxicities grade ≥ 3 (mainly infections, deep vein thrombosis, and fatigue) within the first four months in the high-dose DEX arm (early deaths: 12 vs. 1, $p = 0.003$; grade ≥ 3 toxicity: 52 vs. 35%, $p < 0.001$) [1]. To date, no comparison of high *vs.* low DEX doses has been performed in transplant-eligible NDMM receiving the proteasome inhibitor (PI) bortezomib (BTZ), which is widely applied during induction therapy (IT) prior to stem cell collection and high-dose therapy (HDT).

Therefore, our present analysis retrospectively compared IT regimens from two subsequently conducted multicenter phase III trials applying BTZ (1.3 mg/m^2 on days 1, 4, 8, 11) and doxorubicine (DOXO, 9 mg/m^2 on days 1–4) with

Electronic supplementary material The online version of this article (https://doi.org/10.1038/s41375-018-0195-9) contains supplementary material, which is available to authorized users.

✉ Elias K. Mai
elias.mai@med.uni-heidelberg.de

[1] Department of Internal Medicine V, University Clinic Heidelberg, Heidelberg, Germany
[2] Division of Biostatistics, German Cancer Research Center (DKFZ), Heidelberg, Germany
[3] Department of Hematology and Oncology, Asklepios Hospital Hamburg Altona, Hamburg, Germany
[4] Department of Internal Medicine III, University Medical Center Mainz, Mainz, Germany
[5] Department of Hematology and Oncology, Helios Hospital Berlin Buch, Berlin, Germany
[6] Department of Hematology, University Clinic Essen, Essen, Germany
[7] University Hospital Bonn, Bonn, Germany
[8] Department of Hematology and Oncology, Klinikum Baden Baden, Baden Baden, Germany
[9] Institute of Human Genetics, University of Heidelberg, Heidelberg, Germany
[10] Department of Medicine, Hematology/Oncology, Goethe-University of Frankfurt, Frankfurt, Germany
[11] Department of Hematology and Oncology, Katholisches Krankenhaus Hagen, Hagen, Germany
[12] Medical Clinic, Charité University Medicine Berlin, Berlin, Germany
[13] Department of Internal Medicine I, University Hospital Köln, Köln, Germany
[14] Department of Hematology, Oncology and Immunology, University Hospital Tübingen, Tübingen, Germany
[15] Nationales Centrum für Tumorerkrankungen (NCT) Heidelberg, Heidelberg, Germany

either high-dose DEX (hd-PAD, 40 mg on days 1–4, 9–12, 17–20; 480 mg per cycle) as applied in the German-speaking Myeloma Multicenter Group (GMMG) HD4 trial (05/2005-05/2008, $n = 192$, EudraCT No. 2004-000944-26) vs. low-dose DEX (ld-PAD, 20 mg on days 1–4, 9–12, 17–20; 240 mg per cycle, EudraCT No. 2010-019173-16) as applied in the subsequent GMMG MM5 trial (07/2010-11/2013, $n = 111$). Primary endpoints for these trials have been published previously [2, 3]. The trials were conducted in accordance with the European Clinical Trial Directive, the Declaration of Helsinki and local ethics committees. The maximum age for inclusion was different between the trials (HD4: 65 years vs. MM5: 70 years). Therefore, we included only patients up to 65 years in the MM5 ld-PAD group. BTZ was administered intravenously (IV) in the HD4 trial. In the MM5 trial, the route of administration of BTZ was changed from IV to subcutaneous (SC) in 02/2012. Since SC BTZ resulted in lower overall adverse events (AE), peripheral neuropathy (PN), gastrointestinal and metabolic/nutritional AE compared to IV BTZ [4], only patients receiving IV BTZ were included in the ld-PAD group (MM5) for the current analysis.

The IT period was defined from first IT dose until last IT dose plus 30 days *or* start of stem cell mobilization. The DEX dose was reduced in the MM5 trial because the rates of severe infections during IT (defined as ≥ grade 3 according to the National Cancer Institute Common Terminology Criteria for Adverse Events, CTCAE) were persistently high with the use of hd-PAD compared to vincristine / DOXO / DEX (VAD; VAD 27.6% vs. hd-PAD 27.1%) and infections were a major cause of death during IT in the HD4 trial, with 7 of 12 deaths (58%) being primarily infection-related. Antibiotic prophylaxis was strongly recommended in the HD4 trial from 02/2007 ($n/N = 47/66$ received antibiotic prophylaxis) onwards and throughout the whole MM5 trial ($n/N = 104/111$ received antibiotic prophylaxis). Recommended antibiotic prophylaxis consisted of either ciprofloxacin (500 mg, twice daily) *or* trimethoprim-sulfamethoxazole (800/160 mg, twice daily) during the whole course of IT. Baseline and trial characteristics for the hd-PAD (as applied in the HD4 trial) and ld-PAD (as applied in the MM5 trial) group are displayed in Supplemental Table 1.

The mean applied doses of DEX in the hd-PAD and ld-PAD group were 456.6 vs. 230.5 mg per cycle ($p < 0.001$), respectively. The full DEX dose for three cycles of IT was applied in 63.5 vs. 63.1% ($p = 0.82$) of patients in the hd-PAD and ld-PAD group, respectively. DEX was reduced in 11.5 vs. 8.1% ($p = 0.43$) and interrupted in 5.7 vs. 1.8% ($p = 0.14$) of patients in the hd-PAD and ld-PAD group, respectively. The mean applied doses of BTZ and DOXO during IT were similar between the hd-PAD vs. ld-PAD groups, respectively (BTZ: 14.3 vs. 14.3 mg/m^2, $p = 0.95$ and DOXO: 102.4 vs. 102.2 mg/m^2, $p = 0.73$).

Table 1 Comparison of toxicities between high- and low-dose dexamethasone in bortezomib-containing induction therapies

Variable (n / %)	hd-PAD (HD4 trial)	ld-PAD (MM5 trial)	p Value
	($n = 192$)	($n = 111$)	
Toxicity (≥3°)			
Any AE	116 / 60.4	55 / 49.5	0.07
Non-hematological			
Infections	52 / 27.1	11 / 9.9	**<0.001**
TEE	9 / 4.7	3 / 2.7	0.55
GI	16 / 8.3	8 / 7.2	0.55
PN	13 / 6.8	4 / 3.6	0.31
Hematological			
Leucopenia	12 / 6.2	5 / 4.5	0.61
Anemia	6 / 3.1	8 / 7.2	0.15
Thrombocytopenia	15 / 7.8	10 / 9.0	0.83
Any SAE	79 / 41.1	32 / 28.8	**0.04**
Infection-related SAE	39 / 20.3	13 / 11.7	0.06
Deaths			
Death during IT	4 / 2.1	3 / 2.7	0.71
Death causes (% of deaths)			
Infection	2 / 50.0	2 / 66.7	1.00
PD	1 / 25.0	1 / 33.3	
Unknown	1 / 25.0	—	
Treatment adherence			
Completion of IT	180 / 93.8	103 / 92.8	0.68
Mobilisation therapy	173 / 90.1	102 / 91.9	0.81

Absolute numbers and percent (%) are displayed for each variable. Toxicities are ≥ 3 grade according to CTCAE are compared. p values based on Fisher's exact test. p values < 0.05 indicate significant differences between hd- and ld-PAD

hd high-dose dexamethasone, *ld* low-dose dexamethasone, *PAD* bortezomib, doxorubicin, dexamethasone, *AE* adverse event, *TEE* thromboembolic events, *GI* gastrointestinal, *PN* peripheral neuropathy, *SAE* serious adverse event, *IT* induction therapy, *PD* progressive disease, *CTCAE* common toxicity criteria for adverse events

Bold numbers indicate significant p values.

The incidence of grade ≥3 adverse events (AE), serious AE (SAE), severe infections, thromboembolic events (TEE), peripheral neuropathy (PN), gastrointestinal toxicity and deaths during IT are shown in Table 1. The incidence of severe infections (grade ≥3) and any SAE during IT were significantly lower in the ld-PAD compared to the hd-PAD group (9.9 vs. 27.1%, $p < 0.001$ and 28.8 vs. 41.1%, $p = 0.04$). Accordingly, the incidence of any AE (grade ≥ 3) and infection-related SAE were lower in the ld-PAD vs. hd-PAD arms (49.5 vs. 60.4%, $p = 0.07$ and 11.7 vs. 20.3%, $p = 0.06$). Hematological toxicities were comparable between the ld- and hd-PAD groups (Table 1).

Table 2 Response after induction therapy with either high-dose or low-dose dexamethasone

Respone (*n* / %)	hd-PAD (HD4 trial)	ld-PAD (MM5 trial)	*p* Value
All	(*n* = 192)	(*n* = 111)	
≥PR	144 / 75.0	84 / 75.7	1.0
≥VGPR	69 / 35.9	46 / 41.4	0.39
CR	16 / 8.3	7 / 6.3	0.65
PD	5 / 2.6	1 / 0.9	0.42
Renal impairment	(*n* = 19)	(*n* = 12)	
≥PR	13 / 68.4	7 / 58.4	0.71
≥VGPR	4 / 21.1	5 / 41.7	0.25
CR	1 / 5.3	1 / 8.3	1.0
PD	0 / 0.0	0 / 0.0	—
Adverse cytogenetics	(*n* = 72)	(*n* = 54)	
≥PR	57 / 79.2	40 / 74.1	0.53
≥VGPR	32 / 44.4	27 / 50.0	0.59
CR	8 / 11.1	6 / 11.1	1.0
PD	2 / 2.8	1 / 1.8	1.0

Absolute numbers and percent (%) are displayed for each variable. Adverse cytogenetics are defined as either del17p13 and/or gain 1q21 (≥3 copies) and/or t(4;14). Renal impairment is defined as baseline creatinine ≥ 2 mg/dl. *p* values based on Fisher's exact test. *p* values <0.05 indicate significant differences between hd- and ld-PAD

hd high-dose dexamethasone, *ld* low-dose dexamethasone, *PAD* bortezomib, doxorubicin, dexamethasone, ≥*PR* partial response or better, ≥*VGPR* very good partial response or better, *CR* complete response, *PD* progressive disease

Since antibiotic prophylaxis might influence the rate of infections, we compared patients who received antibiotic prophylaxis between the two PAD groups. However, the incidence of severe infections during IT remained significantly different among patients receiving antibiotic prophylaxis favoring the ld-PAD group (ld-PAD: 10.6% vs. hd-PAD: 27.7%, $p = 0.01$).

Higher DEX doses can increase response to therapy [1]. Comparison of the hd- and ld-PAD group revealed no significant differences in response and progressive disease rates, also in the subgroup with adverse cytogenetics (defined as either deletion17p13 and/or translocation t(4;14) and/or gain1q21 [≥3 copies] [5]; Table 2).

The proportion of patients completing three IT cycles and proceeding to subsequent stem cell mobilization therapy were similar between the ld- and hd-PAD group as was mortality during IT (ld-PAD 3/111 [2.7%] deaths vs. hd-PAD 4/192 [2.1%] deaths, $p = 0.71$).

In line with the results from *Rajkumar and colleagues* [1], we found a lower number of severe infections, overall adverse events and SAE during early therapy. Expectedly, this did not translate into a lower mortality during IT in the ld-PAD group, because a short and fixed number of three IT cycles was applied. Further, the treated cohort was younger in our trials compared to the study from Rajkumar et al. [1]. Regarding age (maximum 65 years) and the route of administration of BTZ (IV only) the two PAD groups in our present analysis were comparable, excluding a bias from these factors. A comparison of hd- and ld-PAD beyond IT, e.g., regarding OS, remains difficult since DEX was only applied during IT and not continuously as with LEN. Further, in the HD4 and MM5 trials, different HDT policies (tandem HDT irrespective of response [HD4] vs. tandem HDT for patients not receiving a near CR (nCR) after first HDT [MM5]) and maintenance therapies (BTZ in the HD4 vs. LEN in the MM5 trial) were applied. Response rates were not affected by the reduced DEX dose.

Severe infections remain a major issue during the initial treatment of MM. A randomized study of continuous antibiotic prophylaxis ($n = 212$) with either ciprofloxacin vs. trimethoprim-sulfamethoxazole vs. observation during the first 2 months of treatment did neither demonstrate a reduction of severe bacterial infections (12.5% vs. 6.8% vs. 15.9%, $p = 0.22$) nor mortality [6]. The TEAMM (Tackling Early Morbidity and Mortality in Myeloma) trial, a large randomized, placebo-controlled study ($n = 977$), compared the prophylactic use of levofloxacin *versus* placebo during the first 12 weeks of treatment in NDMM [7]. The combined primary endpoint, febrile episodes or death from any cause, was significantly improved with the use of levofloxacin (hazard ratio 1.52, $p = 0.002$) with no differences in overall survival after one year ($p = 0.94$). The thrice weekly application of trimethoprim-sulfamethoxazole for pneumocystis prophylaxis was additive with the effects of levofloxacin and the carriage of nosocomial pathogens was not increased by the prophylactic use of levofloxacin. In comparison to the TEAMM trial, our study recommended ciprofloxacin or trimethoprim-sulfamethoxazole twice daily as antibiotic prophylaxis and was neither randomized to compare antibiotic prophylaxis nor placebo-controlled. Patients included in the TEAMM trial had a higher median age of 67 years and only 54% were considered transplant-eligible compared to our study, which included only transplant-eligible patients with a median age of 57 years. Taken together, our results on antibiotic prophylaxis have to be interpreted with caution, whereas the data from the TEAMM trial support the prophylactic use of levofloxacin and trimethoprim-sulfamethoxazole in NDMM.

Taken together, our study demonstrates lower toxicity and maintained efficacy with the use of ld-PAD compared to hd-PAD as IT for transplant-eligible NDMM. Studies applying modern IT regimens including BTZ plus LEN, thalidomide or cyclophosphamide and DEX are needed to confirm these results. This study supports the hypothesis that the application of reduced DEX doses during IT yields

a favorable safety profile while maintaining efficacy in NDMM.

Trial registries

GMMG-HD4: EudraCT No. 2004-000944-26; GMMG-MM5: EudraCT No. 2010-019173-16.

Acknowledgements The GMMG-HD4 trial was supported by the German Federal Ministry of Education and Research (BMBF), Janssen-Cilag-Ortho Biotech, Novartis, Amgen, Chugai, and Roche. The GMMG-MM5 trial was supported by Celgene, Janssen-Cilag, Chugai and The Binding Site.

Compliance with ethical standards

Conflict of interest EKM: Janssen: honoraria, travel grant; Takeda: honoraria, travel grant, advisory board; Celgene: travel grant; Onyx: travel grant; Munidpharma: travel grant. TH: nothing to disclose. UB: Novartis: travel grant. JS: nothing to disclose. HJS: Janssen-Cilag: research funding, honraria, travel grant; Celgene: research funding, honraria, travel grant. MMu: Janssen: advisory board, travel grant; BMS: advisory board, travel grant; Celgene: advisory board; Takeda: advisory board, travel grant; Amgen: advisory board, travel grant. CG: nothing to disclose. UD: nothing to disclose. PB: nothing to disclose. KN: Janssen: advisory board, travel grant; Takeda: advisory board; Celgene: advisory board, travel grant; Boehringer Ingelheim: advisory board; Roche: advisory board; BMS: advisory board; TEVA: advisory board. JH: Amgen: consultancy, honoraria, advisory board, travel grant; Celgene: consultancy, honoraria, advisory board, travel grant; Janssen: honoraria, advisory board, travel grant; Sanofi: research funding; Novartis: honoraria, advisory board, travel grant; BMS: honoraria, travel grant; Takeda: honoraria, travel grant. MSR: Amgen: honoraria, advisory board, research funding, travel grant; Novartis: honoraria, advisory board, research funding, travel grant; Celgene: honoraria, advisory board, travel grant; Janssen: honoraria, advisory board, travel grant; BMS: honoraria, advisory board, travel grant. MMe: Takeda: research funding; Janssen: travel grant; Celgene: travel grant. M-AB: Amgen: travel grant; BMS: travel grant; Janssen: travel grant; Novartis: travel grant, honoraria, research support; Takeda: honoraria. AJ: nothing to disclose. DH: Celgene: advisory board, research funding; Engmab: advisory board, research funding; Takeda: advisory board, travel grant. HM: nothing to disclose. H-WL: nothing to disclose. SC: nothing to disclose. IWB: nothing to disclose. CS: Amgen: honoraria, advisory board, travel grant; BMS: honoraria, advisory board, travel grant; Celgene: honoraria, advisory board, travel grant; Janssen: honoraria, advisory board, travel grant; Novartis: honoraria, advisory board, travel grant; Takeda: honoraria, advisory board, travel grant. KCW: Amgen: honoraria, advisory board, research funding; BMS: honoraria, advisory board; Celgene: honoraria, advisory board, research funding; Janssen: honoraria, advisory board, research funding; Novartis: honoraria, advisory board; Takeda: honoraria, advisory board; Sanofi: research funding. HG: BMS: honoraria, advisory board, research funding, travel grant; Celgene: honoraria, advisory board, research funding, travel grant; Janssen-Cilag: honoraria, advisory board, research funding, travel grant; Novartis: honoraria, advisory board, research funding; Amgen: honoraria, advisory board, travel grant; Takeda: advisory board, travel grant; Chugai: advisory board, research funding.

References

1. Rajkumar SV, Jacobus S, Callander NS, Fonseca R, Vesole DH, Williams ME, et al. Lenalidomide plus high-dose dexamethasone versus lenalidomide plus low-dose dexamethasone as initial therapy for newly diagnosed multiple myeloma: an open-label randomised controlled trial. Lancet Oncol. 2010;11:29–37.
2. Goldschmidt H, Lokhorst HM, Mai EK, van der Holt B, Blau IW, Zweegman S, et al. Bortezomib before and after high-dose therapy in myeloma: long-term results from the phase III HOVON-65/GMMG-HD4 trial. Leukemia. 2017. https://doi.org/10.1038/leu.2017.211.
3. Mai EK, Bertsch U, Dürig J, Kunz C, Haenel M, Blau IW, et al. Phase III trial of bortezomib, cyclophosphamide and dexamethasone (VCD) versus bortezomib, doxorubicin and dexamethasone (PAd) in newly diagnosed myeloma. Leukemia. 2015. https://doi.org/10.1038/leu.2015.80.
4. Merz M, Salwender H, Haenel M, Mai EK, Bertsch U, Kunz C, et al. Subcutaneous versus intravenous bortezomib in two different induction therapies for newly diagnosed multiple myeloma: an interim analysis from the prospective GMMG-MM5 trial. Haematologica. 2015;100:964–9.
5. Neben K, Lokhorst HM, Jauch A, Bertsch U, Hielscher T, van der Holt B, et al. Administration of bortezomib before and after autologous stem cell transplantation improves outcome in multiple myeloma patients with deletion 17p. Blood. 2012;119:940–8.
6. Vesole D, Oken M, Heckler C, Greipp P, Katz M, Jacobus S, et al. Oral antibiotic prophylaxis of early infection in multiple myeloma: a URCC/ECOG randomized phase III study. Leukemia. 2012;26:2517–20.
7. Drayson MT, Bowcock S, Planche T, Iqbal G, Wood J, Raynes K, et al. Tackling early morbidity and mortality in myeloma (TEAMM): assessing the benefit of antibiotic prophylaxis and its effect on healthcare associated infections in 977 patients. Blood. 2017;130:903.

Leukemia (2019) 33:262–266
https://doi.org/10.1038/s41375-018-0201-2

Acute lymphoblastic leukemia

The MCL1-specific inhibitor S63845 acts synergistically with venetoclax/ABT-199 to induce apoptosis in T-cell acute lymphoblastic leukemia cells

Zhaodong Li[1] · Shuning He[1] · A. Thomas Look[1,2]

Received: 29 October 2017 / Revised: 11 June 2018 / Accepted: 19 June 2018 / Published online: 15 July 2018

The mitochondrial cell death pathway is initiated by pro-apoptotic BH3-only effector proteins, such as BIM, BID, NOXA, and PUMA, which activate the multidomain cell death proteins, BAX and BAK [1]. The survival of tumor cells, as well as normal cells, is promoted by anti-apoptotic BCL-2-family members, including BCL-2, BCL-X_L, and MCL1, which bind and sequester BH3-only proteins, thus preventing them from activating BAX and BAK [1]. Cancer cells tend to rely more heavily on anti-apoptotic BCL-2 family proteins because of replicative and other stresses that accompany malignant transformation, and thus are "primed" to undergo apoptosis more readily than normal cells [1]. Small molecules have been developed that mimic the BH3 domain and block binding of endogenous BH3 proteins to a groove on the surface of one or more of the pro-survival proteins. Promising examples are navitoclax/ABT-263, targeting BCL-2, BCL-X_L, and BCL-W, and more recently venetoclax/ABT-199 targeting BCL-2 alone [2]. The most successful of these drugs is the BCL-2 inhibitor venetoclax, which is approved for the treatment of chronic lymphocytic leukemia (CLL) [2, 3] and has shown considerable activity in therapy for other cancers, such as acute myeloid leukemia (AML) [4]. Venetoclax is better tolerated than navitoclax, because it does not bind to BCL-X_L, which is required for the survival of normal platelets [3].

Although T-cell acute lymphoblastic leukemia (T-ALL) is similar in many ways to CLL and AML, it has not responded well to venetoclax or navitoclax BH3 mimetics, presumably because it expresses active pro-survival proteins other than BCL-2, BCL-X_L, and BCL-W. We and others have previously tested venetoclax and navitoclax against a number of human T-ALL cell lines, observing submicromolar activity only in the Loucy cell line, which is thought to represent early thymocyte precursor (or ETP) ALL, a T-ALL subtype with a particularly poor prognosis [5–7]. Venetoclax has been tested in multiple clinical trials (https://clinicaltrials.gov/) and is approved for the treatment of CLL [2, 3], but it has just begun to be tested in patients with T-ALL. This led us to postulate that T-ALL cells might depend upon MCL1, a labile pro-survival member of the BCL-2 family that has been shown to mediate resistance to BCL-2 inhibitors [8, 9]. Thus, inhibitors of MCL1 appear especially attractive for combination with BCL-2 inhibitors for the treatment of T-ALL and other cancers. A new BH3 mimetic, S63845, was recently found to selectively target MCL1, and S63845 has been tested in many preclinical models of human cancer [10], including breast cancer [11], but not in T-ALL. Clinical data for the activity of MCL1 inhibitors, including S63845, have as yet not been reported. Thus, we sought to test the hypothesis that S63845 will actively induce apoptosis in T-ALL cells when given as a single agent, and also that it might produce synergistic effects when used in combination with the BCL-2 inhibitor venetoclax.

Thus, we first tested a panel of 11 T-ALL cell lines for their sensitivity to S63845. Each line was sensitive to S63845 treatment as shown by 50% growth inhibitory

These authors contributed equally: Zhaodong Li and Shuning He

Electronic supplementary material The online version of this article (https://doi.org/10.1038/s41375-018-0201-2) contains supplementary material, which is available to authorized users.

✉ A. Thomas Look
Thomas_Look@dfci.harvard.edu

[1] Department of Paediatric Oncology, Dana-Farber Cancer Institute, Harvard Medical School, Boston, MA 02215, USA

[2] Division of Haematology/Oncology, Boston Children's Hospital, Boston, MA 02215, USA

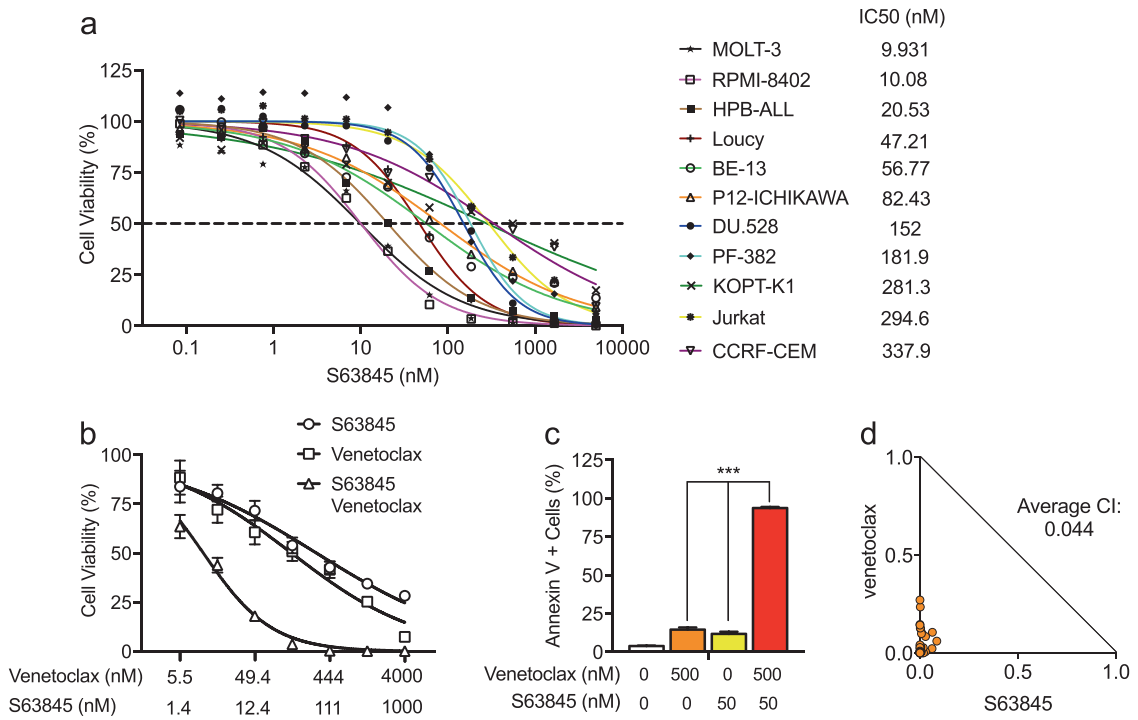

Fig. 1 The MCL1-specific inhibitor S63845 actively kills human T-ALL cells and strongly synergizes with venetoclax. **a** Eleven human T-ALL cell lines were treated with serial dilutions of S63845. Cell viability was determined by Cell-Titer Glo assay after 72 h of treatment. **b** KOPT-K1 cells were treated with serial dilutions of venetoclax or S63845, alone or in combination. Cell viability was determined using Cell-Titer Glo after 48 h of treatment. **c** KOPT-K1 cells were treated with 500 nM venetoclax and 50 nM S63845, alone or in combination. Apoptosis was measured by annexin V/PI staining after 24 h of treatment. **d** Combination treatment of venetoclax and S63845 depicted as normalized isobolograms shows strong synergy between the two BH3 mimetics in KOPT-K1 cells. Calcusyn software was used to analyze combination data to produce the isobolograms normalized to the IC_{50} of each drug. The cells were treated with the following serial dilutions of combination doses: venetoclax, from 5.5 nM to 4000 nM; and S63845, from 1.4 nM to 1000 nM for 48 h. A combination index (CI) of 1 indicates an additive effect, CI < 1 a synergistic effect and CI > 1 antagonism

(IC_{50}) values in a submicromolar range (Fig. 1a). The values for two of the most sensitive cell lines, MOLT-3 and RPMI-8402, were as low as 10 nM. These results indicate that MCL1 plays an important role in maintaining the survival of most T-ALL cells. Consistent with previous studies in AML, chronic myeloid leukemia, and diffuse large B-cell lymphoma cell lines [10], we did not observe correlation between MCL1 protein levels and sensitivity to S63845 in these T-ALL cell lines. Similarly, BCL-2 and BCL-X_L levels did not predict response to S63845 treatment (Supplementary Figure 1). We also tested the activity of A-1210477, another MCL1-specific inhibitor [12], against these T-ALL cell lines in comparison with the activity of S63845. The IC_{50} values for A-1210477 were in the high micromolar range (Supplementary Figure 2), indicating that S63845 is much more potent in a cellular context, even though both drugs exhibit high affinity and specificity for the MCL1 protein in vitro [10, 12].

Next, we tested whether the effects of S63845 were mediated through the activation of apoptosis. Using four relatively sensitive T-ALL cell lines based on IC_{50} values—HPB-ALL, Loucy, MOLT-3, and RPMI-8402—we demonstrated the induction of significant apoptosis by annexin V/propidium iodide (PI) staining after 24 h of treatment with S63845 (Supplementary Figure 3a, b). Western blot analysis after 24 h of treatment with 200 nM S63845 showed appreciable PARP cleavage, a reliable marker of cell apoptosis, in each of these four cell lines (Supplementary Figure 3c). Taken together, these data demonstrate that a representative panel of T-ALL cell lines are sensitive to the S63845 inhibitor and thus depend on MCL1 for cell survival.

The anti-apoptotic BCL-2 family proteins BCL-2, BCL-X_L, and MCL1 can each bind and sequester BH3-only pro-apoptotic proteins, such as BIM, BID, and PUMA [2, 13], raising the possibility that two very specific inhibitors such as venetoclax (BCL-2) and S63845 (MCL1) might act synergistically to kill T-ALL cells. To test this hypothesis, we treated T-ALL cells with serial dilutions of S63845 and venetoclax, either alone or in combination. Our results, shown in Fig. 1b and Supplementary Figure 4 for KOPT-K1 and PF-382 cells, indicate much greater decreased cell viability in cells treated with both agents in combination. This result reflects the induction of apoptosis as shown by annexin V and PI staining (Fig. 1c and Supplementary Figure 5). To determine whether the combined

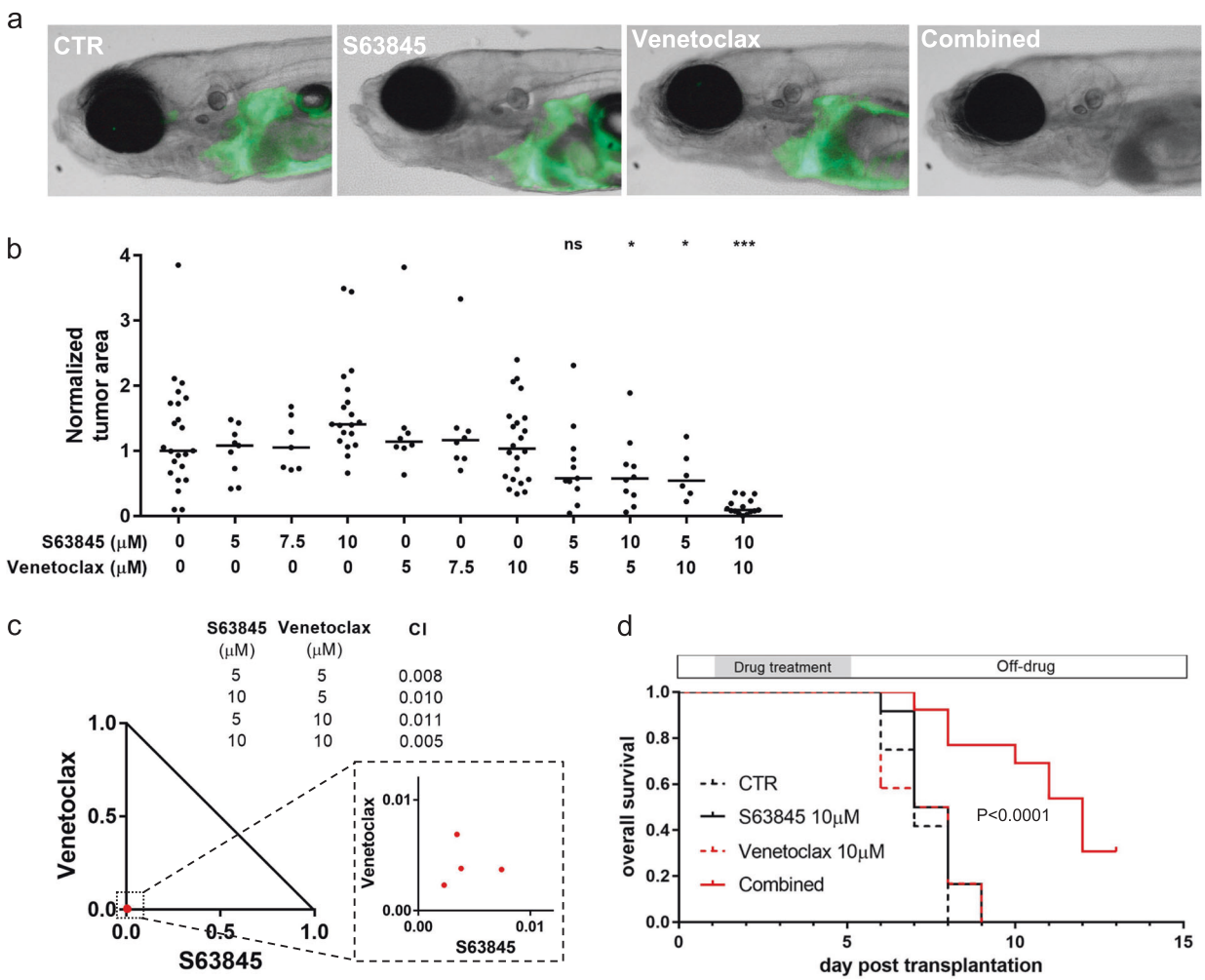

Fig. 2 S63845 strongly synergizes with venetoclax in killing T-ALL cells in vivo. **a** Representative zebrafish embryos transplanted with T-ALL cells isolated from *Tg(rag2:Myc; rag2:EGFP)* zebrafish and treated with vehicle, S63845 (10 μM), venetoclax (10 μM), and the combination of S63845 and venetoclax (10 μM of each). **b** Quantification of GFP-positive leukemic area in zebrafish embryos and compared with vehicle treatment with the two-tailed Welch's *t* test: $*P < 0.05$; $***P < 0.001$. **c** Synergistic effects of S63845 and venetoclax on T-ALL cell kill were analyzed by isobologram analysis. A combination index (CI) of 1 indicates an additive effect, CI < 1 a synergistic effect and CI > 1 indicates antagonism. **d** The combination treatment of S63845 and venetoclax significantly extended the overall survival of T-ALL bearing embryos. Zebrafish embryos transplanted with T-ALL cells were treated as indicated for 4 days, with drug refreshment every 2 days, and then the drugs were removed before feeding was initiated and the developing zebrafish larva were observed for 10 more days ($n = 12$ for CTR, S63845, and venetoclax treatment groups; $n = 13$ for combined treatment group)

effects of S63845 and venetoclax are additive or synergistic, we performed isobologram analysis after 48 h of combination treatment with serial dilutions of S63845 and venetoclax. These agents proved highly synergistic against each of the four T-ALL cell lines tested—KOPT-K1, PF-382, Jurkat, and CCRF-CEM (Fig. 1d and Supplementary Figure 6), with an average combination index (CI) of < 0.25 (a CI of 1 reflects an additive effect, CI < 1 a synergistic effect and CI > 1 indicates antagonism). As shown in Supplementary Figure 7a, protein levels of MCL1 were increased after venetoclax treatment, but venetoclax treatment had little effect on the expression of both BCL-2 and BCL-X_L. Based on the work of Choudhary et al. [9], increased MCL1 levels are expected and may be due to increased MCL1 protein stability after treatment with venetoclax. As observed previously [10], treatment of S63845 also caused upregulation of MCL1 levels with little effect on expression levels of BCL-2 and BCL-X_L (Supplementary Figure 7b). Thus, the compensatory upregulation of MCL1 suggests a molecular basis for both the lack of response of most T-ALL lines to venetoclax treatment [5] and for the synergy between S63845 and venetoclax in these T-ALL cell lines.

To assess the potential toxicity of this combination in normal cells in vivo, a critical concern when testing such agents for possible use in patients, we turned to our zebrafish model of T-ALL [14]. We first added each of the two compounds at graded doses as single agents to the fish water of normal 3-day-old zebrafish embryos. After

4 days of treatment, we determined that the maximum tolerable dose of both S63845 and venetoclax was 10 μM. Developmental defects of multiple organs including the liver, swim bladder, and gastrointestinal tract were observed in embryos treated with 15 μM S63845 (Supplementary Figure 8). However, we found no evidence of toxicity in embryos treated with 10 μM S63845 alone or in combination with 10 μM venetoclax, indicating that the combination is well tolerated at these dosages by healthy tissues in vivo.

To determine the anti-T-ALL activity of S63845 and venetoclax, we harvested green fluorescent protein (GFP)-labeled zebrafish T-ALL cells from 3-month-old *Tg(rag2:Myc; rag2:EGFP)* transgenic zebrafish [14], and intravenously injected these T-ALL cells into 2-day-old zebrafish embryos [15]. One day after injection, embryos bearing GFP-labeled T-ALL cells were treated with S63845, venetoclax or vehicle (dimethyl sulfoxide), each added to the fish water as single agents. After 4 days of treatment, the GFP-labeled T-ALL cells had proliferated and disseminated throughout the recipient embryos that were treated with vehicle, S63845, or venetoclax (Fig. 2a, b). To further investigate why the Myc-driven zebrafish T-ALL cells are insensitive to MCL1 inhibition as a single agent, we treated zebrafish embryos with S63845 and venetoclax, either as single agents or in combination. Then we analyzed lysates of whole embryos by western blotting, and we observed marked compensatory upregulation of both BCL-2 and MCL1 protein levels upon treatment with either drug (Supplementary Figure 9). BCL-2 was not upregulated in response to S63845 in T-ALL cell lines treated in vitro, accounting for the apoptotic response of T-ALL cell lines but not zebrafish thymocytes in vivo to treatment with S63845 as a single agent. There are not sufficient cells in the zebrafish embryos to study only the thymocytes by western blotting, but at least at the whole embryo level, compensatory upregulation appears to explain resistance to treatment with each drug as single agent.

The major impact of S63845 and venetoclax was evident when they were administered together. At 10 μM S63845 plus 10 μM venetoclax, this combination greatly reduced the number of leukemic cells in the vast majority of embryos after 4 days of treatment (Fig. 2a, b). Importantly, the synergistic anti-T-ALL effects of S63845 plus venetoclax were documented in vivo at several different dosage levels by isobologram analysis (Fig. 2c), indicating that MCL1 and BCL-2 inhibitors are synergistic at multiple dosage levels leading to T-ALL cell apoptosis in vivo with acceptable tolerance by normal cells.

To address the effects of treatment on survival of the transplanted embryos, we removed the drugs after treating the embryos with S63845 and venetoclax as single agents or combinations for a period of 4 days and then started feeding the embryos and observed them an additional 10 days (Fig. 2d). We found that treatment with the combination of S63845 and venetoclax significantly extended the overall survival of T-ALL bearing embryos, whereas single drug treatment with either drug had no impact survival. The treatments did not affect the viability of leukemia-free fish, excluding possibility that the fish treated with the combination died from toxicity of the treatment they received (Supplementary Figure 10). In addition, the fish treated with the combination exhibited growth of the GFP-labeled T-ALL cells after stopping the drugs and prior to their death. The last four fish were killed at day 13 with rapidly growing, disseminated GFP-positive T-ALL cells for humane reasons (Fig. 2d).

In conclusion, our study demonstrates that the MCL1-specific inhibitor S63845 actively kills human T-ALL cells as a single agent and acts synergistically with venetoclax to more potently induce apoptosis. These drugs were well tolerated in the zebrafish model when given alone and in combination. Interestingly, neither drug alone could effectively kill transplanted T-ALL cells growing in vivo, apparently owing to upregulation of MCL1 and BCL-2 levels in response to treatment with either drug. However, combined administration of S63845 and venetoclax led to profound synergistic activity against T-ALL in vitro and in vivo without appreciable toxicity even at doses that greatly reduced transplanted T-ALL cells in zebrafish embryos. Our results indicate that the newly developed MCL1-specific inhibitor S63845 warrants testing in clinical trials for relapse/refractory patients with T-ALL, both alone and in combination with venetoclax to simultaneously inhibit both MCL1 and BCL-2.

Acknowledgements We thank John Gilbert of editorial assistance; Megan W. Martel and Kassandra Bacon for zebrafish husbandry. This work was funded by NIH grant 1R35 CA210064-01 (A.T.L). Z.L. was supported by David Abraham Fellowship Award and Alex's Lemonade Stand Foundation Young Investigator Award. S.H. was supported by Alex's Lemonade Stand Foundation Young Investigator Award.

Compliance with ethical standards

Conflict of interest The authors declare that they have no conflict of interest.

References

1. Bhola PD, Letai A. Mitochondria-judges and executioners of cell death sentences. Mol Cell. 2016;61:695–704.
2. Delbridge AR, Grabow S, Strasser A, Vaux DL. Thirty years of BCL-2: translating cell death discoveries into novel cancer therapies. Nat Rev Cancer. 2016;16:99–109.
3. Souers AJ, Leverson JD, Boghaert ER, Ackler SL, Catron ND, Chen J, et al. ABT-199, a potent and selective BCL-2 inhibitor, achieves antitumor activity while sparing platelets. Nat Med. 2013;19:202–8.
4. Pan R, Hogdal LJ, Benito JM, Bucci D, Han L, Borthakur G, et al. Selective BCL-2 inhibition by ABT-199 causes on-target cell death in acute myeloid leukemia. Cancer Discov. 2014;4:362–75.
5. Anderson NM, Harrold I, Mansour MR, Sanda T, McKeown M, Nagykary N, et al. BCL-2-specific inhibitor ABT-199 synergizes strongly with cytarabine against the early immature LOUCY cell line but not more-differentiated T-ALL cell lines. Leukemia. 2014;28:1145–8.
6. Chonghaile TN, Roderick JE, Glenfield C, Ryan J, Sallan SE, Silverman LB, et al. Maturation stage of T-cell acute lymphoblastic leukemia determines BCL-2 versus BCL-XL dependence and sensitivity to ABT-199. Cancer Discov. 2014;4:1074–87.
7. Peirs S, Matthijssens F, Goossens S, Van de Walle I, Ruggero K, de Bock CE, et al. ABT-199 mediated inhibition of BCL-2 as a novel therapeutic strategy in T-cell acute lymphoblastic leukemia. Blood. 2014;124:3738–47.
8. Bojarczuk K, Sasi BK, Gobessi S, Innocenti I, Pozzato G, Laurenti L, et al. BCR signaling inhibitors differ in their ability to overcome Mcl-1-mediated resistance of CLL B cells to ABT-199. Blood. 2016;127:3192–201.
9. Choudhary GS, Al-Harbi S, Mazumder S, Hill BT, Smith MR, Bodo J, et al. MCL-1 and BCL-xL-dependent resistance to the BCL-2 inhibitor ABT-199 can be overcome by preventing PI3K/AKT/mTOR activation in lymphoid malignancies. Cell Death Dis. 2015;6:e1593.
10. Kotschy A, Szlavik Z, Murray J, Davidson J, Maragno AL, Le Toumelin-Braizat G, et al. The MCL1 inhibitor S63845 is tolerable and effective in diverse cancer models. Nature. 2016;538:477–82.
11. Merino D, Whittle JR, Vaillant F, Serrano A, Gong JN, Giner G, et al. Synergistic action of the MCL-1 inhibitor S63845 with current therapies in preclinical models of triple-negative and HER2-amplified breast cancer. Sci Transl Med. 2017;9:pii: eaam7049.
12. Leverson JD, Zhang H, Chen J, Tahir SK, Phillips DC, Xue J, et al. Potent and selective small-molecule MCL-1 inhibitors demonstrate on-target cancer cell killing activity as single agents and in combination with ABT-263 (navitoclax). Cell Death Dis. 2015;6:e1590.
13. Potter DS, Letai A. To prime, or not to prime: that is the question. Cold Spring Harb Symp Quant Biol. 2016;81:131–40.
14. Gutierrez A, Pan L, Groen RW, Baleydier F, Kentsis A, Marineau J, et al. Phenothiazines induce PP2A-mediated apoptosis in T cell acute lymphoblastic leukemia. J Clin Invest. 2014;124:644–55.
15. He S, Lamers GE, Beenakker JW, Cui C, Ghotra VP, Danen EH, et al. Neutrophil-mediated experimental metastasis is enhanced by VEGFR inhibition in a zebrafish xenograft model. J Pathol. 2012;227:431–45.

Leukemia (2019) 33:266–270
https://doi.org/10.1038/s41375-018-0213-y

Acute lymphoblastic leukemia

Acute lymphoblastic leukemia as a clonally unrelated second primary malignancy after multiple myeloma

Ibrahim Aldoss[1] · Marzia Capelletti[2] · Jihye Park[2] · Romanos Sklavenitis Pistofidis[2] · Raju Pillai[3] · Tracey Stiller[4] · James F. Sanchez[5] · Stephen J. Forman[1] · Irene M. Ghobrial[2] · Amrita Krishnan[5]

Received: 5 March 2018 / Revised: 15 June 2018 / Accepted: 20 June 2018 / Published online: 19 July 2018

These authors contributed equally: Ibrahim Aldoss, Marzia Capelletti, Irene M. Ghobrial, Amrita Krishnan

✉ Irene M. Ghobrial
Irene_Ghobrial@DFCI.harvard.edu

✉ Amrita Krishnan
akrishnan@coh.org

[1] Department of Hematology and Hematopoietic Cell Transplantation, Gehr Family Center for Leukemia Research, City of Hope, Duarte, CA, USA

[2] Division of Hematological Malignancies, Department of Medical Oncology, Dana-Farber Cancer Institute, 450 Brookline Avenue, Boston, MA 02115, USA

[3] Department of Pathology, City of Hope, Duarte, CA, USA

[4] Department of Information Science, City of Hope, Duarte, CA, USA

[5] The Judy and Bernard Briskin Center for Multiple Myeloma Research, City of Hope, Duarte, CA, USA

Abstract

Multiple myeloma (MM) patients have an 11-fold increased risk of developing myeloid neoplasms compared to the general population; however, acute lymphoblastic leukemia (ALL) is rarely observed. Given that both MM and the majority of ALL are of B cell origin, this raises the question of whether ALL in patients with MM arises from the same clone. We report 13 cases of B-cell ALL following therapy for MM. The interval from MM diagnosis to ALL onset was 5.4 years (range 3.3–10). The median age at the time of ALL diagnosis was 60 years (range 43–67). MM therapy included immunomodulatory agents in all patients and autologous hematopoietic cell transplantation in 10 (77%) patients preceding ALL diagnosis. ALL genetics showed a normal karyotype, TP53 mutation/deletion, and monosomy 7 or 7q deletion in 5, 3, and 2 cases, respectively. Analysis of paired samples of MM and ALL using whole exome sequencing demonstrated that the malignancies arose from different clones. Thus, ALL as a second primary malignancy following MM is not clonally related but could potentially represent a therapy-related leukemia.

Second primary malignancies (SPM) remain a concern for patients with multiple myeloma (MM), especially as MM survival improves [1]. Large population-based studies suggest that the risk of an SPM is 26% higher in MM patients compared with the general population [2]. The etiology of these SPMs remains unclear, but theories implicate host, genetic, and MM treatment factors [1].

The incidence of hematologic malignancies as an SPM in MM is 0.8–3.1% [3–5]. The majority of cases are myelodysplastic syndrome (MDS) and acute myeloid leukemia (AML), but acute lymphoblastic leukemia (ALL) has been occasionally reported [6–8]. The IFM2005 study and the CALGB100104 trial of lenalidomide maintenance following hematopoietic cell transplantation (HCT) reported three cases and one case of ALL, respectively [6, 7]. However, no details on their clonal origin were reported. Because both B-cell ALL and MM originate from abnormal post-germinal center B-cells, this fact raises the question of whether post-MM ALL represents a clonal dedifferentiation from a more indolent MM to an aggressive ALL, or a therapy-related leukemia triggered by the genotoxic effect of MM therapy [8, 9]. The transformation of mature B-cell lymphomas to ALL has been reported, with related clones in follicular lymphoma and unrelated clones in chronic lymphocytic leukemia [10, 11]. Other possibilities include the coincident development of two unrelated malignancies or the presence of a germline mutation predisposing the patient to several malignancies as noted in MM with other malignancies [12].

Herein, we describe a single-institution series of ALL cases as SPM after MM, and we examine the clonal relationship between these two B-cell malignancies in a subset of cases to further explore their relationship.

We retrospectively reviewed all consecutive cases of adult ALL treated at City of Hope between 2000 and 2017, and we identified cases that had an antecedent MM diagnosis. This study was approved by the Institutional Review Board.

Six paired MM and ALL samples were obtained when available, and whole exome sequencing was performed to assess the clonal relationship between the two malignancies. Pre-autologous HCT mobilized stem cells and a bone marrow biopsy at remission were used as a surrogate for germline controls in 4 and 1 cases, respectively. These were the only available samples from the deceased subjects in the study. Genomic DNA was extracted with QIAamp DNA Micro Kit (Qiagen; Venlo, Netherlands) according to manufacturer instructions. The libraries were prepared with TruSeq Exome Library Prep Kit (Illumina; San Diego, CA, USA) and 100 ng of genomic DNA. Two or three libraries were pooled together and sequenced on Illumina HiSeq 4000 in high-output mode with 100 paired-end reads to obtain a minimum coverage of 100× per sample. Sequencing data were analyzed using the pipelines of the Broad Institute of Harvard and MIT (Firehose, www.broadinstitute.org/cancer/cga), resulting in BAM files aligned to hg19 with calibrated quality scores [13]. We used MuTect within the Firehose framework to call somatic mutations in tumor aspirates [13]. We filtered out potential artefactual OxoG mutations as well as somatic single nucleotide variations (SSNVs) and indels present in a panel of normal samples. To estimate somatic copy number alteration, we used ReCapSeg (http://gatkforums.broadinstitute.org/categories/recapseg-documentation), which calculated proportional coverage for each target region and then normalized each segment using the median proportional coverage in a panel of normal (PON) samples sequenced with the same capture technology. The sample was projected to a hyperplane defined by the PON, and the tumor copy-ratio was estimated. These copy-ratio profiles were segmented with CBS [14]. To estimate allelic copy number, germline heterozygous sites in the normal sample were called via GATK Haplotype Caller [15, 16]. Then, the contribution of each homologous chromosome was assessed via reference and alternate read counts at the germline heterozygous sites. Finally, we segmented the allele specific copy ratios using PSCBS [14]. Copy ratios and the force-called SSNVs and indels were used to estimate the sample purity, ploidy, and cancer cell

fraction by ABSOLUTE [13]. To assess mutation clonality in matched samples, we used PHYLOGIC to perform clustering of ABSOLUTE CCFs, as previously described [13].

Demographic, disease, and treatment characteristics were reported using descriptive statistics; median and range for continuous variables; and frequency and percent for categorical variables. Leukemia free survival (LFS) and overall survival (OS) were calculated from the date of ALL diagnosis using the Kaplan-Meier product-limit method. All analyses were performed using SAS version 9.4 (SAS Institute; Cary, NC, USA). Data were locked for analysis on 8 January 2018.

We identified 13 (1.3%) cases of ALL preceded by MM out of 1022 adults diagnosed with ALL; all had a B-cell phenotype. The median age at the time of ALL diagnosis was 60 years (range 43–67), and 62% were male. The median interval of latency from MM diagnosis to ALL diagnosis was 5.4 years (range 3.3–10.0), and the interval from the date of autologous HCT to ALL diagnosis was 4.3 years (range 2.7–6.0) (Table 1).

All patients received immunomodulatory drugs (IMiDs) as part of MM therapy before ALL onset, including six patients who were treated with lenalidomide and eight who were treated with thalidomide. Bortezomib was administered to 7 (54%) patients, chemotherapy (either standard dose or high dose [$n = 10$, 77%]) was given to 12 (92%) patients, and 3 (23%) patients had prior involved field radiation. Eleven patients received maintenance therapy, the majority with lenalidomide. Three (23%) patients had evidence of active MM at the time of ALL diagnosis.

With respect to ALL, the median white blood cell (WBC) count at the time of diagnosis was 2000/μL (range, 1.2k-29k). The hyperCVAD regimen was used as ALL initial induction in the majority of patients ($n = 12$, 92%), and 85% of all patients achieved complete remission (CR). Eight patients (62%) subsequently underwent allogeneic HCT. The median follow-up for all patients was 16.2 months (range 5.7–118.0). One-year event free survival and OS from the time of ALL diagnosis were both 77% (95% CI 44–92%).

Six paired MM and ALL DNA samples, as well as germline controls for all the cases but one, were available and underwent whole exome sequencing. One paired sample was excluded from downstream analysis because of lack of germline control. The mean coverage was 229X for all sequenced samples. We investigated the number and spectrum of somatic mutations and copy number alterations (CNA) in both neoplasms, and we did not identify any differences compared to publicly available datasets. Only three matched samples were further analyzed by PHYLOGIC due to low purity (<15%) for two of the matched samples. Phylogenetic analysis clearly indicated that

Table 1 Patient characteristics

Category	Number (percent or range). $N = 13$.
Median age at ALL diagnosis	60 (43–67)
Sex	
Female	5 (38.5)
Male	8 (61.5)
Race	
White	5 (38.5)
Hispanic	6 (46.1)
Other/unknown	2 (15.4)
MM subtype	
IgG	6 (46.2)
IgM	0 (0)
IgA	4 (30.8)
Light chain MM	3 (23.1)
MM cytogenetics	
Unavailable	5 (38.5)
Normal karyotype	6 (46.2)
TP53 deletion	1 (7.7)
Monosomy 13 and trisomy 4, 5, 9 and 15	1 (7.7)
MM therapy	
IMiDs	13 (100)
Bortezomib	7 (53.8)
Chemotherapy	12 (92.3)
Radiation	3 (23.1)
Maintenance therapy for MM	
Yes	11 (84.6)
No	2 (15.4)
IMiDs for MM	
thalidomide	8 (61.5)
lenladomide	6 (46.2)
AutoHCT for MM	
Yes	10 (76.9)
No	3 (23.1)
MM relapsed	
Yes	6 (46.2)
No	7 (53.8)
Median time of latency	
From MM diagnosis	5.4 (3.3–10.0)
From autoHCT	4.3 (2.7–6.0)
MM active at the time of ALL	
Yes	3 (23.1)
No	10 (76.9)
WBC at ALL presentation	2 (1.2–29)
ALL phenotype	
B-cell	13 (100)
T-cell	0 (0)
ALL cytogenetics	
Normal karyotype	5 (38.5)
TP53 deletion/mutation	3 (23.1)
Monosomy 7 or 7q deletion	2 (15.4)
Trisomy 8	1 (7.7)
Hyperdiploidy	1 (7.7)
add(9)(q34),del(14)(q22q32),inv(20)(q13)	1 (7.7)

ALL acute lymphoblastic leukemia, *autoHCT* autologous hematopoietic cell transplantation, *IMID* immunomodulatory drug, *MM* multiple myeloma, *WBC* white blood cell

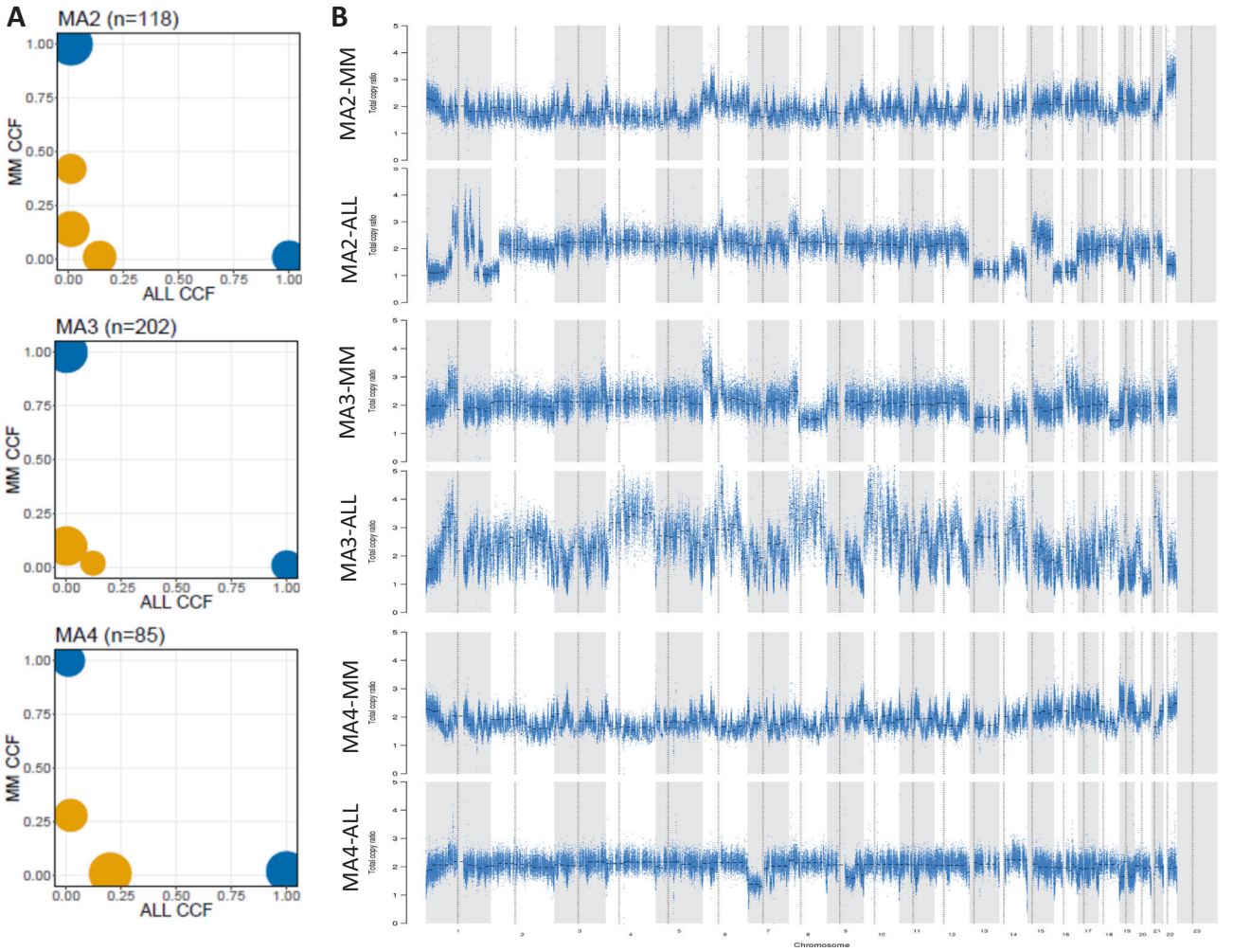

Fig. 1 ALL as a second primary malignancy is clonally unrelated to preceding MM. **a** Cancer cell fraction (CCF) for clusters of SSNVs detected in MM and ALL samples from the same patient. Mutations were clustered by CCF for each pair of samples using PHYLOGIC. Clonal (navy blue) SSNVs were defined as events having ≥0.9 CCF in both samples. Subclonal (yellow) SSNVs were defined as events having <0.9 CCF in samples. Size of circles indicated the fraction of SSNVs. Mutations having ≥0.9 detection power in both samples are shown, and clusters with <3 mutations are excluded. At the top of each plot are reported the ID of the patient and the number of mutations considered in the plot. In the *x* axis are represented clonal (navy blue) and subclonal (yellow) mutations identified in ALL, while on the *y* axis are shown mutations found in MM; **b** Copy number alteration in paired samples showing distinctive variations. The panel of each sample visualizes the total copy number ratio of each chromosome

the two neoplasms are clonally unrelated, with clonal and subclonal mutations and CNAs unique to each malignancy (Fig. 1).

Secondary hematologic malignancies are a known risk in patients with myeloma, and they mainly comprise cases of AML or MDS [17]. Originally, this finding was ascribed to the use of melphalan as a mainstay of MM therapy, and more recently, the use of lenalidomide, especially following autologous HCT [7]. On the other hand, ALL has rarely been noted.

Here, we have described a case series of ALL as an SPM after MM, encompassing the clinical and genetic features of this cohort. We have shown that all patients in this cohort were treated with IMiDs for their myeloma and the majority also underwent autologous HCT before ALL onset.

Both MM and the majority of ALL are B-cell malignancies, and their sequential development in the same patient may suggest an MM clonal dedifferentiation into a more aggressive form of B-cell malignancy, such as B-cell ALL. Nonetheless, our exome sequencing analysis of paired DNA samples from 6 cases of this cohort illustrated that the neoplasms were clonally unrelated, contradicting this hypothesis. On the other hand, therapy-related ALL has been described as a complication of exposure to cytotoxic therapies in the course of unrelated primary malignancies [8, 9]. Our ALL cohort was enriched with the TP53

mutation/deletion, as well as other genetic features observed frequently in therapy-related myeloid neoplasms, such as complex karyotype, monosomal karyotype and 7q deletion [18]. Therefore, we postulate that a subset of these cases could be therapy-related leukemia as the result of prior MM treatment, presenting as a B-cell ALL phenotype rather than the more frequently seen myeloid phenotype. Further evaluation of a larger cohort is required, and it would be of interest to expand this study to therapy-related acute myeloid leukemia and myelodysplastic syndrome.

Acknowledgements The Biostatistics and Molecular Pathology Cores at City of Hope were supported by the National Institutes of Health under award number P30CA033572. The content is solely the responsibility of the authors and does not necessarily represent the official views of the National Institutes of Health.

Author contributions Designed studies: I.A., M.C., I.G., A.K., data collection: I.A., performed experiments: M.C., analysis: I.A., T.S., M.C., J.P., R.S.P., J.S., I.G., writing: I.A., J.S., A.K., review and editing: all authors.

Compliance with ethical standards

Conflict of interest I.A. serves on the speakers' bureau for Jazz Pharmaceuticals. A.K. is a consultant and serves on the speakers' bureau for Janssen, Celgene, Takeda, and Onyx. The remaining authors declare that they have no conflict of interest.

References

1. Razavi P, Rand KA, Cozen W, Chanan-Khan A, Usmani S, Ailawadhi S. Patterns of second primary malignancy risk in multiple myeloma patients before and after the introduction of novel therapeutics. Blood Cancer J. 2013;3:e121.
2. Jonsdottir G, Lund SH, Bjorkholm M, Turesson I, Hultcrantz M, Porwit A, et al. The impact of prior malignancies on second malignancies and survival in MM patients: a population-based study. Blood Adv. 2017;1:2392–8.
3. Barlogie B, Tricot G, Haessler J, van Rhee F, Cottler-Fox M, Anaissie E, et al. Cytogenetically defined myelodysplasia after melphalan-based autotransplantation for multiple myeloma linked to poor hematopoietic stem-cell mobilization: the Arkansas experience in more than 3000 patients treated since 1989. Blood. 2008;111:94–100.
4. Usmani SZ, Sexton R, Hoering A, Heuck CJ, Nair B, Waheed S, et al. Second malignancies in total therapy 2 and 3 for newly diagnosed multiple myeloma: influence of thalidomide and lenalidomide during maintenance. Blood. 2012;120:1597–1600.
5. Rollison DE, Komrokji R, Lee JH, Hampras S, Fulp W, Fisher K, et al. Subsequent primary malignancies among multiple myeloma patients treated with or without lenalidomide. Leuk Lymphoma. 2017;58:560–8.
6. Attal M, Lauwers-Cances V, Marit G, Caillot D, Moreau P, Facon T, et al. Lenalidomide maintenance after stem-cell transplantation for multiple myeloma. N Engl J Med. 2012;366:1782–91.
7. McCarthy PL, Owzar K, Hofmeister CC, Hurd DD, Hassoun H, Richardson PG, et al. Lenalidomide after stem-cell transplantation for multiple myeloma. N Engl J Med. 2012;366:1770–81.
8. Aldoss I, Dagis A, Palmer J, Forman S, Pullarkat V. Therapy-related ALL: cytogenetic features and hematopoietic cell transplantation outcome. Bone Marrow Transplant. 2015;50:746–8.
9. Tang G, Zuo Z, Thomas DA, Lin P, Liu D, Hu Y, et al. Precursor B-acute lymphoblastic leukemia occurring in patients with a history of prior malignancies: is it therapy-related? Haematologica. 2012;97:919–25.
10. Kishimoto W, Shirase T, Chihara D, Maeda T, Arimoto-Miyamoto K, Takeoka T, et al. Double-hit lymphoma with a feature of follicular lymphoma concurrent with clonally related B lymphoblastic leukemia: a preference of transformation for the bone marrow. J Clin Exp Hematop. 2012;52:113–9.
11. Chakhachiro Z, Yin CC, Abruzzo LV, Aladily TN, Barron LL, Banks HE, et al. B-lymphoblastic leukemia in patients with chronic lymphocytic leukemia: a report of four cases. Am J Clin Pathol. 2015;144:333–40.
12. Dilworth D, Liu L, Stewart AK, Berenson JR, Lassam N, Hogg D. Germline CDKN2A mutation implicated in predisposition to multiple myeloma. Blood. 2000;95:1869–71.
13. Manier S, Park J, Capelletti M, Bustoros M, Freeman S, Ha G, et al. Whole-exome sequencing of cell-free DNA and circulating tumor cells in multiple myeloma. Nat. Commun. 2018; In press. Volume 9: p. 1691.
14. Venkatraman ES, Olshen AB. A faster circular binary segmentation algorithm for the analysis of array CGH data. Bioinformatics. 2007;23:657–63.
15. DePristo MA, Banks E, Poplin R, Garimella KV, Maguire JR, Hartl C, et al. A framework for variation discovery and genotyping using next-generation DNA sequencing data. Nat Genet. 2011;43:491–8.
16. McKenna A, Hanna M, Banks E, Sivachenko A, Cibulskis K, Kernytsky A, et al. The Genome Analysis Toolkit: a MapReduce framework for analyzing next-generation DNA sequencing data. Genome Res. 2010;20:1297–303.
17. Landgren O, Thomas A, Mailankody S. Myeloma and second primary cancers. N Engl J Med. 2011;365:2241–2.
18. Smith SM, Le Beau MM, Huo D, Karrison T, Sobecks RM, Anastasi J, et al. Clinical-cytogenetic associations in 306 patients with therapy-related myelodysplasia and myeloid leukemia: the University of Chicago series. Blood. 2003;102:43–52.

Leukemia (2019) 33:271–274
https://doi.org/10.1038/s41375-018-0224-8

Chronic myeloproliferative neoplasms

AKT activation is a feature of *CALR* mutant myeloproliferative neoplasms

Chunling Fu[1,2] · Qiang Jeremy Wen[2] · Christian Marinaccio[2] · Te Ling[2] · Wei Chen[1,2] · Marinka Bulic[2] · Terra Lasho[3] · Ayalew Tefferi[3] · John D. Crispino[2] · Kailin Xu[1]

Received: 11 March 2018 / Revised: 6 July 2018 / Accepted: 11 July 2018 / Published online: 6 August 2018

Among the driver mutations in the MPNs, the mechanism by which *CALR* mutations activate JAK/STAT signaling is unique in that the novel C-terminus of *CALR* mutant proteins binds directly to MPL leading to constitutive activation [1, 2]. *CALR* mutants have also been shown to activate the MAPK pathway [3]. Whether *CALR* mutants further activate PI3K/AKT signaling is controversial, with several studies reporting a lack of (or modest) activation [2, 4], but another demonstrating potent activation [5]. The former studies relied upon transduction of Ba/F3 TpoR cells with *CALR* mutant alleles whereas the latter probed the pathway in cells lines with megakaryocytic potential. Moreover, the extent to which PI3K/AKT signaling is a target in *CALR* mutant MPNs has been debated, with at least one study reporting that inhibitors of this pathway do not synergize with ruxolitinib [2].

To address the discrepancy, we assayed for activation of JAK/STAT and AKT in multiple settings. First, we overexpressed the *CALR* type 1 (del52) and type 2 (ins5) mutants in primary murine c-kit$^+$ bone marrow progenitors and cultured the cells for 48 h. We observed enhanced activation of both STAT5 and AKT (Fig. 1a). Next we transplanted bone marrow transduced with *CALRdel52* mutant or empty vector to irradiated recipient mice and assessed AKT activation. Both intracellular flow and western blots of spleen cells revealed increase in p-AKT (Figs. 1b, c). Finally, we assayed for total and phospho-AKT in primary *CALR* mutant MPN samples. We observed robust increase in AKT phosphorylation in patient derived CD34$^+$ cells (Fig. 1d and Supplementary Table 1). This was accompanied by an increase in cyclinD3 consistent with the increased proliferation of the *CALR* mutant cells. These cells also expressed MPL, consistent with the manner in which *CALR* mutants activate signaling (Fig. 1d).

We previously reported that inhibition of AKT activity with the selective AKT inhibitor MK-2206 resulted in reduced growth of MPLW515L expressing cells both in vitro and in vivo, suggesting that this pathway is a therapeutic target in ET and PMF [6]. To determine whether *CALR* mutant expressing cells are similarly dependent on PI3K/AKT signaling, we treated CD34$^+$ cells from PMF patients or healthy individuals with MK-2206. We found that *CALR* mutant cells were susceptible to AKT inhibition and more sensitive than healthy progenitor cells in colony assays (Figs. 1e, f). Of note, the differential effect was much more significant for megakaryocyte colonies (Fig. 1f) than for myeloid colonies (Fig. 1e), consistent with a reliance of megakaryocytes on MPL signaling. Finally, while the level of p-AKT was higher in bone marrow cells from mice transplanted with *CALRdel52* expressing cells compared to those with empty vector, the degree of inhibition was similar (Fig. 1g).

MK-2206 was well tolerated in healthy C57Bl/6 mice with no evidence of myelosuppression or impaired hematopoiesis [6]. To determine the extent to which the drug suppressed thrombocytosis and megakaryopoiesis induced by mutant *CALR*, we transplanted *CALRdel52* mutant expressing hematopoietic progenitor cells into irradiated

Electronic supplementary material The online version of this article (https://doi.org/10.1038/s41375-018-0224-8) contains supplementary material, which is available to authorized users.

✉ John D. Crispino
j-crispino@northwestern.edu

✉ Kailin Xu
lihmd@163.com

[1] Blood Disease Institute, Xuzhou Medical University, Xuzhou, China

[2] Division of Hematology/Oncology, Northwestern University, Chicago, IL, USA

[3] Division of Hematology/Oncology, Mayo Clinic, Rochester, MN, USA

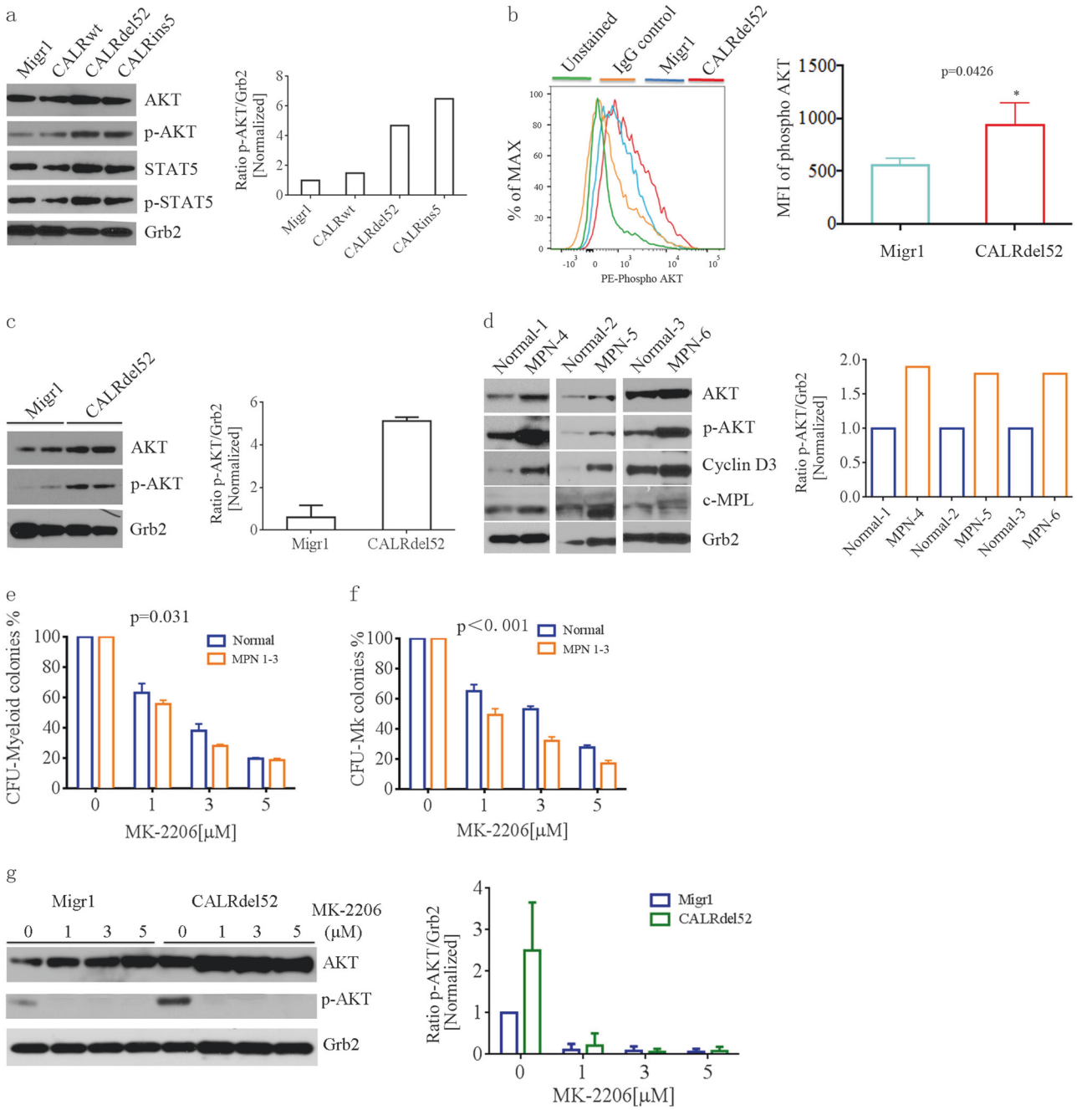

Fig. 1 PI3K/AKT signaling is active in *CALR* mutant MPNs. **a** Western blot and quantitation of STAT5 and PI3K/AKT activation (pS473) in murine bone marrow cells expressing wild-type *CALR*, *CALRdel52* or *CALR*ins5 mutants versus those with Migr1 empty vector. **b** AKT phosphorylation as measured by intracellular flow cytometry of spleen cells from recipients of bone marrow cells transduced with *CALRdel52* or empty vector, 20 weeks post transplantation. (Right) Mean fluorescence intensity (MFI) of the flow cytometry data. Mean ± SD is shown for $n = 2$ Migr1 and 3 *CALRdel52* samples. $*p < 0.05$. **c** Western blot and quantitation of pS473 and total AKT levels in spleen cells from recipients of bone marrow cells transduced with *CALRdel52* or empty vector. **d** Western blots and quantitation of AKT phosphorylation in human MPN patient samples. **e**, **f** CFU-Myeloid (**e**) and CFU-MK (**f**) assays for *CALR* mutant MPN versus healthy $CD34^+$ cells treated with MK-2206. $n = 3$; the samples correspond to MPN-1, MPN-2, and MPN-3. The responses are significantly different as measured by 2-way ANOVA, $p = 0.031$ (**e**) and $p < 0.001$ (**f**). **g** Western blot and quantitation of AKT phosphorylation in bone marrow cells harvested from mice transplanted with *CALRdel52* expressing cells cultured in the presence of increasing doses of MK-2206 in vitro for 24 h. Bar graphs depict mean ± SD. $n = 3$ biological replicates. Grb2 is included as a loading control for the western blots

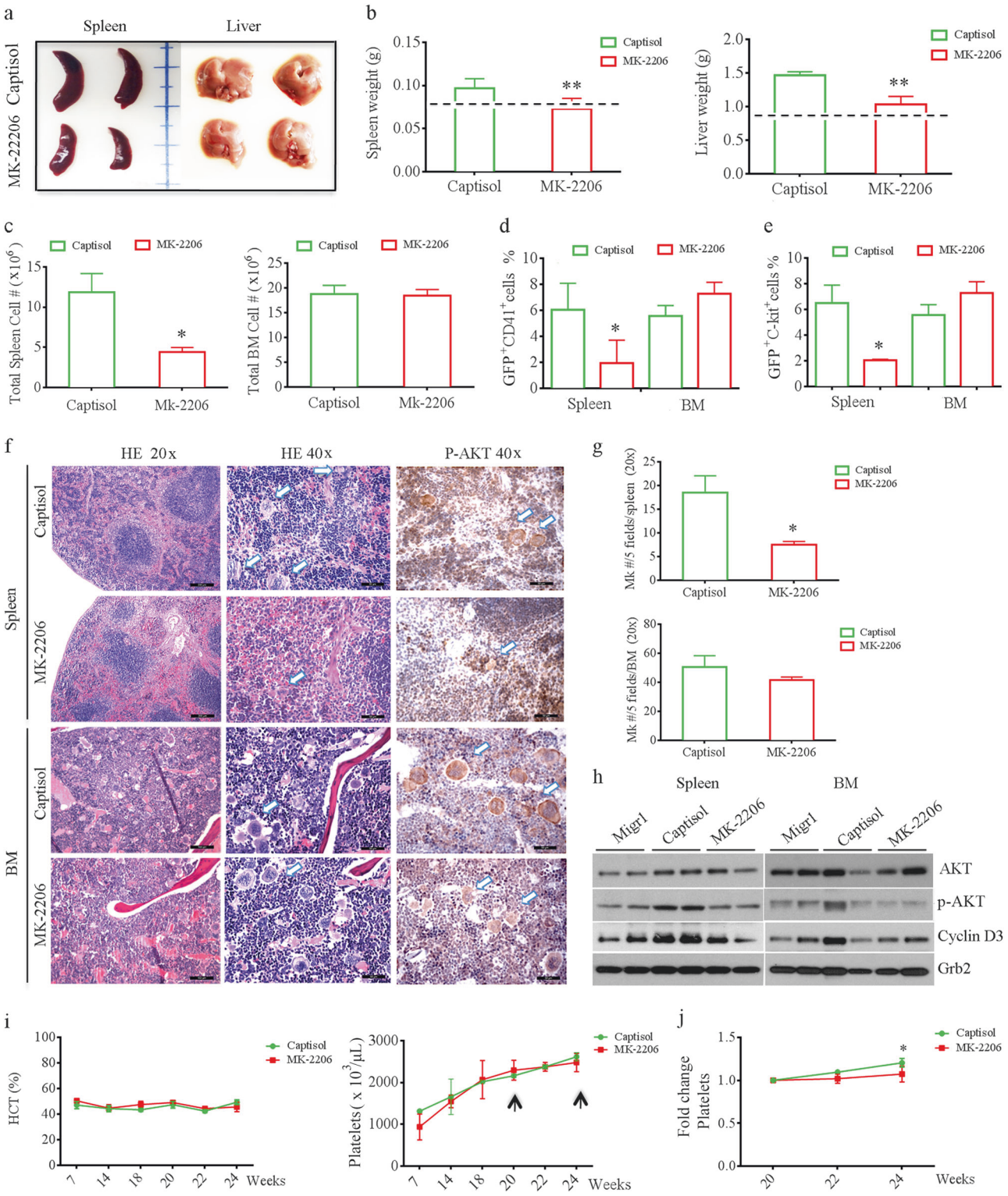

recipients. Recipients developed splenomegaly, hepatomegaly and thrombocytosis by 14 weeks (Fig. 2a, f), similar to previous reports [1, 4, 7]. Treatment of mice with MK-2206 20 weeks post-transplant led to significant reductions in spleen and liver weights (Fig. 2b), as well as the total cell count in the spleen, but not the bone marrow (Fig. 2c). The absence of a striking bone marrow effect could be the result of a greater dependence of hematopoiesis in the spleen in this animal model. We also observed decreases in the percentages of c-kit$^+$ and CD41$^+$ cells and the number of

◀ **Fig. 2** AKT is a therapeutic target in *CALR* mutant MPNs. Captisol (vehicle) or 120 mg/kg MK-2206 were administered to *CALRdel52* mice by oral gavage for 4 weeks, 5 days a week, beginning 20 weeks post-transplant. Hematopoiesis was analyzed at 24 weeks post-transplant. **a** Images of spleens and livers from captisol versus MK-2206 treated animals. **b** Spleen and liver weights from mice treated with captisol or MK-2206. Typical spleen and liver weights of healthy mice are depicted by a dotted line. **c** Total spleen and bone marrow cell counts with captisol or MK-2206 treatment. **d**, **e** Percentages of GFP^+ $CD41^+$ (**d**) or GFP^+ $c\text{-}kit^+$ (**e**) cells in the spleen or bone marrow of mice following captisol or MK-2206 treatment. **f** Hematoxylin/eosin stained spleen and sternum bone marrow sections from mice treated with captisol or MK-2206. Scale bars = 100 µm (20×) and 50 µm (40×). Original magnification 200× and 400×. **g** Quantitation of the numbers of megakaryocytes in the bone marrow and spleen of treated mice. **h** Western blot evaluating the levels of AKT, p-AKT and cyclinD3 in treated mice. Grb2 is included as a loading control. **i** Hematocrit and platelet counts of mice at different time points post-transplant. Mice were treated with MK-2206 beginning at 20 weeks. Left and right arrows indicate the initiation and cessation of treatment, respectively. **j** Fold change in platelet counts during MK-2206 therapy. $^*p < 0.05$; $^{**}p < 0.01$

megakaryocytes in the spleen, but not the bone marrow (Fig. 2d–g). Analysis of p-AKT levels revealed decreases in both total spleen and bone marrow cells (Fig. 2h). This inhibition of AKT signaling failed to reduce the degree of thrombocytosis (Fig. 2i), but it did prevent a further increase in the platelet count (Fig. 2j). MK-2206 also had no significant effect on the hematocrit or other peripheral blood parameters (Fig. 2i and data not shown). Given the modest effect of AKT inhibition as a single agent, we next combined MK-2206 with ruxolitinib. We observed synergy in inhibition of colony formation from murine hematopoietic progenitor cells expressing *CALRdel52* (Supplementary Table 2). Of note, CFU-Mk assays revealed a much stronger synergy of MK-2206 with ruxolitinib than myeloid colonies. These results suggest that although MK-2206 showed modest activity as a single agent, combining it with ruxolitinib may enhance the anti-tumor effect of both drugs, especially against cells that are dependent upon MPL.

Although ruxolitinib shows similar efficacy patients with any of the three driver mutations [8], it has limited use in that most patients progress or become intolerant within 2–3 years [9]. Therefore, novel agents to enhance or follow ruxolitinib are needed. Here we demonstrate that AKT signaling is indeed increased in *CALR* mutant MPN patients and further reveal that AKT is a therapeutic target in this group of patients. With development of new PI3K/AKT inhibitors, inhibition of this pathway should be pursued in combination with ruxolitinib for the group of patients with *CALR* mutations.

Acknowledgements The authors thank Zan Huang for the *CALR* mutant expressing plasmids. This study was supported by NIH grant HL112792.

Compliance with ethical standards

Conflict of interest The authors declare that they have no conflict of interest.

References

1. Elf S, Abdelfattah NS, Chen E, Perales-Paton J, Rosen EA, Ko A, et al. Mutant calreticulin requires both its mutant c-terminus and the thrombopoietin receptor for oncogenic transformation. Cancer Discov. 2016;6:368–81.
2. Chachoua I, Pecquet C, El-Khoury M, Nivarthi H, Albu RI, Marty C, et al. Thrombopoietin receptor activation by myeloproliferative neoplasm associated calreticulin mutants. Blood. 2016;127:1325–35.
3. Kollmann K, Warsch W, Gonzalez-Arias C, Nice FL, Avezov E, Milburn J, et al. A novel signalling screen demonstrates that CALR mutations activate essential MAPK signalling and facilitate megakaryocyte differentiation. Leukemia. 2017;31:934–44.
4. Marty C, Pecquet C, Nivarthi H, El-Khoury M, Chachoua I, Tulliez M, et al. Calreticulin mutants in mice induce an MPL-dependent thrombocytosis with frequent progression to myelofibrosis. Blood. 2016;127:1317–24.
5. Han L, Schubert C, Kohler J, Schemionek M, Isfort S, Brummendorf TH, et al. Calreticulin-mutant proteins induce megakaryocytic signaling to transform hematopoietic cells and undergo accelerated degradation and Golgi-mediated secretion. J Hematol Oncol. 2016;9:45.
6. Khan I, Huang Z, Wen Q, Stankiewicz MJ, Gilles L, Goldenson B, et al. AKT is a therapeutic target in myeloproliferative neoplasms. Leukemia. 2013;27:1882–90.
7. Shide K, Kameda T, Yamaji T, Sekine M, Inada N, Kamiunten A, et al. Calreticulin mutant mice develop essential thrombocythemia that is ameliorated by the JAK inhibitor ruxolitinib. Leukemia. 2017;31:1136–44.
8. Hobbs GS, Rozelle S, Mullally A. The development and use of janus kinase 2 inhibitors for the treatment of myeloproliferative neoplasms. Hematol Oncol Clin North Am. 2017;31:613–26.
9. Pardanani A, Tefferi A. Definition and management of ruxolitinib treatment failure in myelofibrosis. Blood Cancer J. 2014;4:e268.

Leukemia (2019) 33:275–278
https://doi.org/10.1038/s41375-018-0243-5

Cytogenetics and molecular genetics

Characterization of an X-chromosome-linked telomere biology disorder in females with *DKC1* mutation

Elina A. M. Hirvonen[1] · Saara Peuhkuri[1] · Anna Norberg[2] · Sofie Degerman[2] · Katariina Hannula-Jouppi[3,4] · Hannamari Välimaa[5] · Outi Kilpivaara[1] · Ulla Wartiovaara-Kautto[6]

Received: 18 June 2018 / Revised: 13 July 2018 / Accepted: 19 July 2018 / Published online: 5 September 2018

Dyskeratosis congenita (DC) caused by mutations in genes implicated in telomere biology is an inherited syndrome affecting multiple tissues. Clinical severity and the spectrum of symptoms are variable but classically patients present with significant hemato-immunological, odontological, mucosal, and dermatological disturbances [1]. This is due to defective telomere maintenance in rapidly renewing tissues, causing shortened telomeres and DC-like manifestations in the respective organ. Other common clinical features are hepatic, pulmonal, ophthalmologic, and neuropsychiatric health problems. DC also predisposes patients to cancer, especially hematological malignancies and squamous cell carcinomas of the head and neck [2]. Remarkably, the risk of myelodysplastic syndrome (MDS) is over 500-fold in comparison to healthy individuals [2]. Hence, early recognition of all patients with DC or other telomere biology disorder (TBD) is crucial.

One of the genes linked to DC is *DKC1*, located on chromosome X and encoding a highly conserved protein dyskerin. Dyskerin is an essential nucleolar protein, which maintains stability of the human telomerase RNA (TERC) by interacting with H/ACA consensus sequence in TERC. Pathogenic mutations in *DKC1* result in a dysfunctional protein, leading to reduced levels of TERC, decreased telomerase activity, and premature telomere shortening in males [3]. Dyskerin has a role also in controlling ribosome biogenesis [3]. X-chromosome inactivation (XCI) silences transcription from one of the two X chromosomes in female cells to balance expression dosage between males and females. The inactivation process is sometimes incomplete in human tissues, thus up to one-third of X-chromosomal genes may be expressed from both the active and silenced X chromosomes [3]. There are few reports on females with DKC1 mutation [4–6]. Here, we report results of detailed molecular and clinical investigation of three symptomatic sisters aiming at enlightening X-linked TBD in females.

We recently identified two brothers with a novel *DKC1* mutation c.1218_1219insCAG, p.(Asp406_Ser407insGln) resulting in short telomeres and manifestation of DC [6]. Three female siblings (mother and two aunts of the brothers) were studied at the Department of Hematology in Helsinki University Hospital Comprehensive Cancer Center in 2016–2017 amid hematologic consultation of the brothers. Clinical examination and sampling for extended routine analyses, as well as research laboratory analyses, were performed for all the females. Informed consents were

These authors contributed equally: Outi Kilpivaara, Ulla Wartiovaara-Kautto.

Electronic supplementary material The online version of this article (https://doi.org/10.1038/s41375-018-0243-5) contains supplementary material, which is available to authorized users.

✉ Outi Kilpivaara
outi.kilpivaara@helsinki.fi

✉ Ulla Wartiovaara-Kautto
ulla.wartiovaara-kautto@hus.fi

[1] Genome-Scale Biology/Research Programs Unit, and Department of Medical and Clinical Genetics/Medicum, University of Helsinki, Helsinki, Finland

[2] Department of Medical Biosciences, Medical and Clinical Genetics, Umeå University, Umeå, Sweden

[3] Department of Dermatology and Allergology, University of Helsinki and Helsinki University Central Hospital, Helsinki, Finland

[4] Folkhälsan Institute of Genetics, Helsinki, and Molecular Neurology/Research Programs Unit, University of Helsinki, Helsinki, Finland

[5] Department of Virology, University of Helsinki and Department of Oral and Maxillofacial Surgery, University of Helsinki and Helsinki University Hospital, Helsinki, Finland

[6] Department of Hematology, Helsinki University Hospital Comprehensive Cancer Center and University of Helsinki, Helsinki, Finland

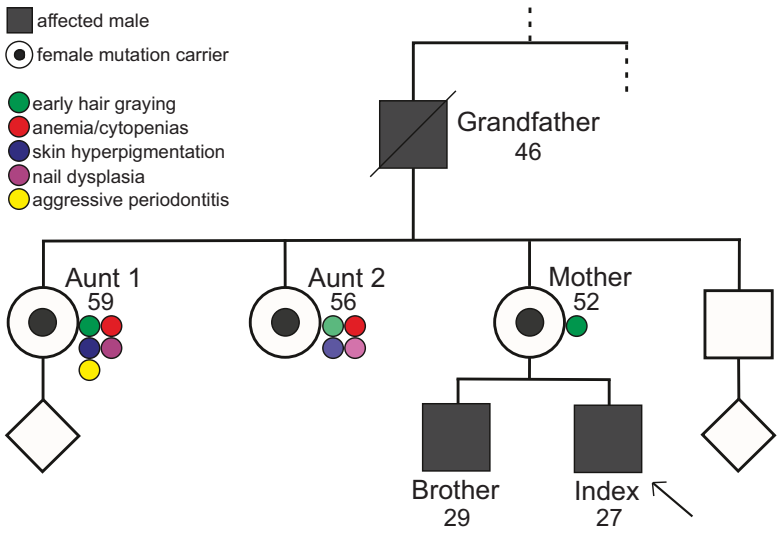

Laboratory findings (reference values; F=female)	Mother	Aunt 1	Aunt 2
Hb(F: 134-167 g/L)	141	114	109
Eryt(F: 4.25-5.70 E12/L)	4.19	3.44	3.46
Reticulocytes(0.7-2.3%)	1.2	2.7	1.2
MCV(82-98 fl)	97	98	95
Leuk(3.4-8.2 E9/L)	9.0	6.1	4.2
Neut(1.5-6.7 E9/L)	6.6	3.7	2.4
Lymph(1.3-3.6 E9/L)	1.5	1.9	1.3
B-cells(CD19+) (0.08-0.62 E9/L)	0.23	0.19	0.27
T-cells(CD3+) (0.75-2.76 E9/L)	1.14	1.22	0.84
T-cells(CD4+) (0.404-1.612 E9/L)	0.502	0.744	0.268
T-cells(CD8+) (0.22-1.13 E9/L)	0.59	0.50	0.58
NK-cells(0.08-0.72 E9/L)	0.10	0.18	0.17
HbF(<1.0%)	7.4	2.9	2.0

Fig. 1 Pedigree, clinical features, and laboratory findings of c.1218_1219insCAG, p.(Asp406_Ser407insGln) mutation carrier females. In the pedigree, circles with dots represent mutation carrier females and dark squares represent males with DC. Index case is marked with an arrow. Ages at time of examination are shown. Grandfather died traumatically at 46 years of age. Colored dots denote the clinical features; darker tone of a colored dot refers to more severe symptoms. Green: early hair graying; red: anemia/cytopenias; blue: skin hyperpigmentation; purple: nail dysplasia; yellow: aggressive periodontitis. Abnormal laboratory findings are shown in red in the table

obtained from participating individuals. This study was conducted in accordance with the principles of Helsinki Declaration and was approved by the Ethics Committee of Helsinki University Hospital (#206/13/03/03/2016). Detailed descriptions of the study subjects and analyses are presented in Fig. 1, Supplementary Table 1, and in the Supplementary information.

All the females were confirmed to be heterozygous *DKC1* mutation carriers by Sanger sequencing. In order to study X-inactivation in various tissues, we compared the *DKC1* expression levels and distribution of wild type (WT) and mutant alleles in blood, buccal mucosa, tongue, and Epstein-Barr virus (EBV)-transformed lymphocytes using Sanger sequencing and droplet digital PCR (ddPCR). ddPCR is superior to traditional quantitative PCR as it is more sensitive and allows absolute quantitative measurement of RNA expression [7] (Fig. 2). With ddPCR, the mutant allele burden in blood was 0% in the mother, 45% in aunt 1, and 5% in aunt 2. Also, buccal mucosa and tongue samples showed varying amounts of mutant *DKC1* allele expression in all the females (Fig. 2). Although we observed both mutant and WT alleles to be present, e.g., in blood samples, it is possible, or even likely, that signals come from different cells expressing either WT or mutant *DKC1*, and not both. The EBV-transformed lymphocytes showed extremely high overall *DKC1* expression, >98% being WT *DKC1* (Supplementary Figure 1). Dyskerin expression has been reported to be similar in EBV-transformed lymphoblastoid cells in mutation carrying females vs. controls [8]. Here, we show that the extremely high *DKC1* expression in transformed cells does not reflect the situation in naïve cells. This is not surprising as such, since dyskerin expression increases with malignant transformation [9]. Consequently, EBV-transformed lymphoblastoid cells should not be used in evaluation of telomere functionality.

The telomere lengths (TL) were measured in whole blood by a quantitative PCR-based method [10]. Two out of the three females (mother and the aunt 1) had shortened telomeres compared to age-matched controls (Supplementary Figure 2). The telomeres in the two brothers were previously shown to be very short (<5th percentile) and are depicted in the same figure for comparison. According to the literature, there is not a strict relationship between TL and severity of symptoms at an individual level [11]. Families have been reported where individuals display variable symptoms and differences in telomere lengths even though they carry the same mutation [12, 13]. Also, gene/mutation-specific effect on TL is unclear. The brothers with extremely short TL had clear clinical mucocutaneous and immunological manifestations of DC. However, in the females, the correlation of TL with clinical presentation was less obvious and inquired more detailed investigation. The expression of *DKC1* measured by ddPCR in blood correlated better with, e.g., anemia.

In *DKC1*-linked TBD, skewed X-inactivation has been thought to function especially well in hematopoietic tissues [6] and protect females from hematologic symptoms. In our study, both mutant and WT *DKC1* are expressed in blood in

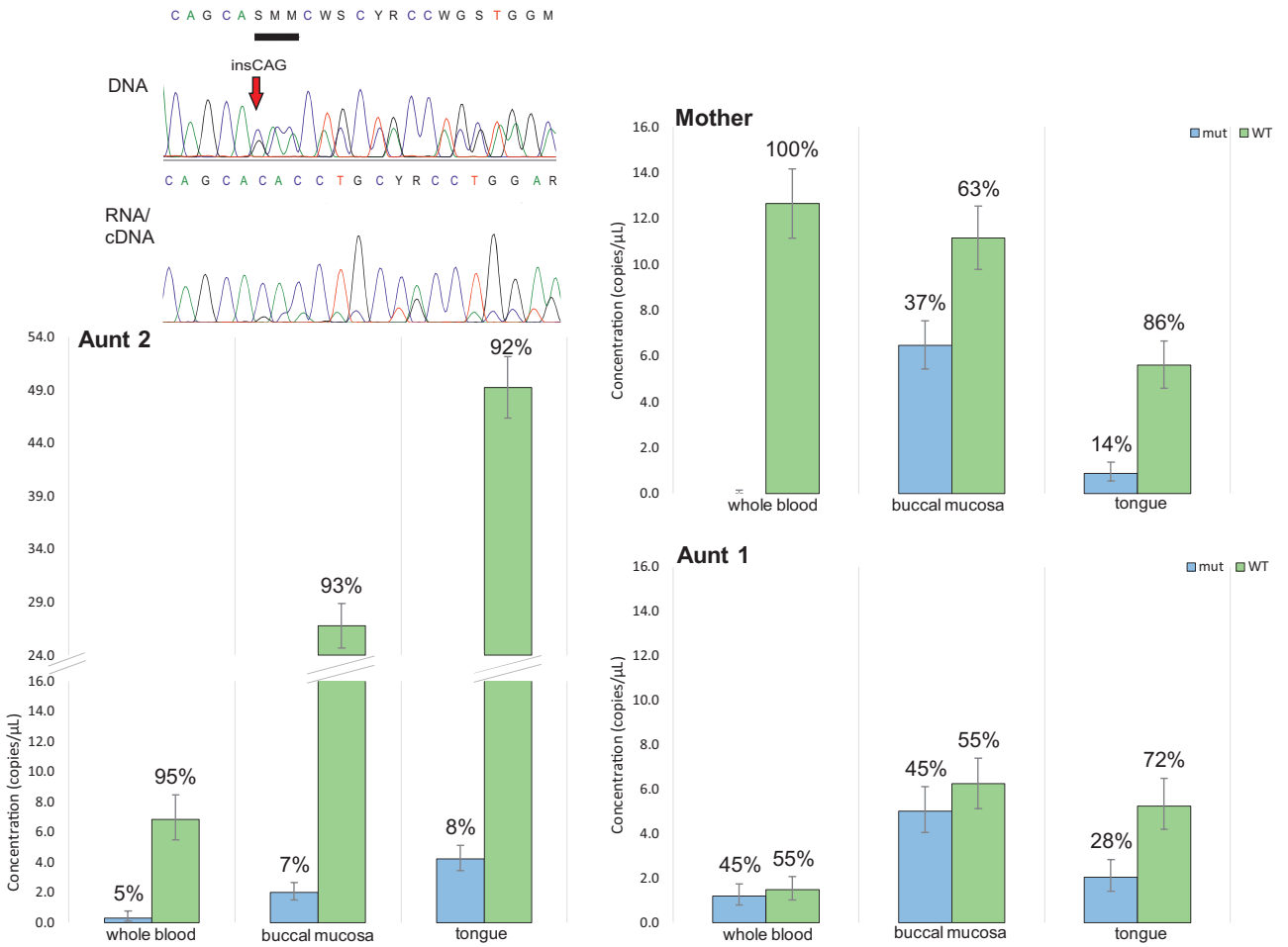

Fig. 2 Expression levels and distribution of mutant (mut; blue) and wild type (WT; green) alleles in blood, buccal mucosa, and tongue detected with ddPCR duplex assay. Sanger sequencing chromatogram from buccal mucosa of aunt 1 exemplifies how this method is not suitable for absolute quantification. Insertion of three nucleotides in DNA sequence is marked with an arrow. Concentrations (copies/µl) of mut and WT cDNA copies reverse-transcribed from tissue sample RNA from all the females are shown (note different *y*-axis scales). The error bars represent Poisson 95% confidence intervals

two out of three females. They both have suffered from marginal macrocytic anemia for some years. Bone marrow biopsy examination in aunt 2 showed mild hypoplasia and explained for the findings in the blood picture. It is highly likely that also aunt 1 has corresponding findings in her bone marrow, although sampling has been postponed due to more urgent ophthalmologic procedures. Interestingly, and in accordance with previous findings in patients with DC, all the carrier females had elevated levels of hemoglobin F potentially suggesting for stress hematopoiesis and bone marrow failure syndrome.

It has been speculated whether clonal hematopoiesis can precede myeloid malignancy in patients with DC. Thus, potential development of clonal hematopoiesis in the two aunts with anemia was investigated by a myeloid next-generation sequencing panel. Neither of the patients had any somatic mutations in genes involved in myeloid neoplasms, corresponding well to recent findings [14]. A long-term surveillance of genomic evolution in DC patients is still indicated aiming at early detection of MDS.

Regarding other clinical findings in our study patients, at least two of the three females had abnormal early graying of hair and nail atypia (Supplementary Table 1). Also, subtle dermatologic features indicative of DC were present in both aunts (Supplementary Figure 3). However, they lacked the typical reticular pigmentation of the head and neck.

In summary, we demonstrate here that in rare diseases such as TBDs, careful clinical and molecular examination of one family can significantly increase our knowledge on disease features. Despite X-linked inheritance, two out of three females in this study fulfill the diagnostic criteria for DC- or DC-like syndrome [1]. In conjunction with widening the clinical spectrum of *DKC1*-linked TBD in women, we are also able to reveal the molecular roots of patients' symptoms. Whether the unique distribution pattern of mutant and WT *DKC1* in distinct tissues arises by co-

incidence or is a controlled biological phenomenon, remains to be investigated. DC is a multi-organ disease with high incidence of developing malignancies [2]. Since the health problems in female *DKC1* mutation carriers may also be significant, the identification, registration, and careful follow-up of these individuals is called for.

Acknowledgements This study was funded by grants from Academy of Finland (#274474, #312492, and #284538), Helsinki University Hospital Comprehensive Cancer Center Research Funding, Cancer Society of Finland, Signe and Ane Gyllenberg Foundation, and Väre Foundation for Pediatric Cancer Research. We are grateful to patients who participated and thus made this study possible. We thank Lotta Honkala, Pihla Siipola, and Annukka Ruokolainen for excellent technical assistance, and FIMM Technology Center for Sanger sequencing services.

Author contributions EAMH and SP conducted the molecular laboratory experiments and analyzed the results (except the telomere analysis). AN and SD conducted the telomere length analysis and analyzed the results. KH-J and HV are responsible for the dermatological and odontological and oral mucosal examination and interpretation, respectively. OK and UW-K designed the study, participated in the analyses, and finalized the manuscript. All authors participated in drafting the manuscript and have read and approved the final manuscript.

Compliance with ethical standards

Conflict of interest The authors declare that they have no conflict of interest.

References

1. Savage SA. Beginning at the ends: telomeres and human disease. F1000Res. 2018;7:524 https://doi.org/10.12688/f1000research.14068.1.
2. Alter BP, Giri N, Savage SA, Rosenberg PS. Cancer in the National Cancer Institute inherited bone marrow failure syndrome cohort after fifteen years of follow-up. Haematologica. 2018;103:30–9.
3. Tukiainen T, Villani AC, Yen A, Rivas MA, Marshall JL, Satija R, et al. Landscape of X chromosome inactivation across human tissues. Nature. 2017;550:244–8.
4. Devriendt K, Matthijs G, Legius E, Schollen E, Blockmans D, Van Geet C, et al. Skewed X-chromosome inactivation in female carriers of dyskeratosis congenita. Am J Hum Genet. 1997;60:581–7.
5. Vulliamy TJ, Knight SW, Dokal I, Mason PJ. Skewed X-inactivation in carriers of X-linked dyskeratosis congenita. Blood. 1997;90:2213–6.
6. Trotta L, Norberg A, Taskinen M, Beziat V, Degerman S, Wartiovaara-Kautto U, et al. Diagnostics of rare disorders: whole-exome sequencing deciphering locus heterogeneity in telomere biology disorders. Orphanet J Rare Dis. (in press).
7. Hindson BJ, Ness KD, Masquelier DA, Belgrader P, Heredia NJ, Makarewicz AJ, et al. High-throughput droplet digital PCR system for absolute quantitation of DNA copy number. Anal Chem. 2011;83:8604–10.
8. Xu J, Khincha PP, Giri N, Alter BP, Savage SA, Wong JM. Investigation of chromosome X inactivation and clinical phenotypes in female carriers of DKC1 mutations. Am J Hematol. 2016;91:1215–20.
9. Fernandez-Garcia I, Marcos T, Munoz-Barrutia A, Serrano D, Pio R, Montuenga LM, et al. Multiscale in situ analysis of the role of dyskerin in lung cancer cells. Integr Biol (Camb). 2013;5:402–13.
10. Cawthon RM. Telomere measurement by quantitative PCR. Nucleic Acids Res. 2002;30:e47.
11. Vulliamy TJ, Kirwan MJ, Beswick R, Hossain U, Baqai C, Ratcliffe A, et al. Differences in disease severity but similar telomere lengths in genetic subgroups of patients with telomerase and shelterin mutations. PLoS ONE. 2011;6:e24383.
12. Alder JK, Hanumanthu VS, Strong MA, Dezern AE, Stanley SE, Takemoto CM, et al. Diagnostic utility of telomere length testing in a hospital-based setting. Proc Natl Acad Sci USA. 2018;115:E2358–65.
13. Norberg A, Rosen A, Raaschou-Jensen K, Kjeldsen L, Moilanen JS, Paulsson-Karlsson Y, et al. Novel variants in Nordic patients referred for genetic testing of telomere-related disorders. Eur J Hum Genet. 2018;26:858–67.
14. Kirschner M, Maurer A, Wlodarski MW, Ventura Ferreira MS, Bouillon AS, Halfmeyer I, et al. Recurrent somatic mutations are rare in patients with cryptic dyskeratosis congenita. Leukemia. 2018. https://doi.org/10.1038/s41375-018-0125-x.